Raty, M., Peippo, J., Greve, T. and Callesen, H. (2005): Respiration rates of individual bovine in vitro-produced embryos measured with a novel, non-invasive and highly sensitive microsensor system. Reproduction, 130, 669–679.
43) Lopes, A.S., Greve, T. and Callesen, H. (2007): Quantification of embryo quality by respirometry. Theriogenology, 67, 21–31.
44) Bard, A.J. and Mirkin, M.V. (2001): Scanning Electrochemical Microscopy, Marcel Dekker Inc., New York.
45) Shiku, H., Shiraishi, T., Ohya, H., Matsue, T., Abe, H., Hoshi, H. and Kobayashi, M. (2001): Oxygen consumption of single bovine embryos probed with scanning electrochemical microscopy. Anal. Chem., 73, 3751–3758.
46) Abe, H., Shiku, H., Aoyagi, S. and Hoshi, H. (2004): In vitro culture and evaluation of embryos for production of high quality bovine embryos. J. Mamm. Ova Res., 21, 22–30.
47) Abe, H. (2007): A non-invaseve and sensitive method for measureing cellular respiration with a scanning electrochemical microscopy to evaluate embryo quality. J. Mamm. Ova Res., 24, 70–78.
48) Yokoo, M., Ito-Sasaki, T., Shiku, H., Matsue, T. and Abe, H. (2008) Multiple analysis of respiratory activity in the identical oocytes by applying scanning electrochemical microscopy. Trans. Materials Res. Soc. JPN., 33, 763–766.
49) Mikkelesen, A.L., Smith, S.D. and Lindenberg, S. (1999): In vitro maturation of human oocytes from regularly menstruating women may be successful without follicle stimulating hormone priming. Hum. Reprod., 14, 1847–1851.
50) Wynn, P., Piction, H.M., Krapez, J.A., Rutherford, A.J., Balen, A.H. and Gosden, R.G. (1998): Pretreatment with follicle stimulating hormone promotes the numbers of human oocytes reaching metaphase II by in vitro maturation. Hum. Reprod., 13, 3132–3138.
51) Sato, E. and Koide, S. (1987): Biochemical transmitters regulating the arrest and resumption of meiosis in oocytes. Int. Rev. Cytol., 106, 1–33.
52) Jin, Z.X., Ock, S.A., Tan, S.L. and Chian, R.C. (2005): What is the smallest size of follicle to respond to human chorionic gonadotropin injestion? Fertl. Steril., 84, S147.
53) Chian, R.C., Buckett, W.M., Turandi, T. and Tan, S.L. (2000): Prospective randomized study of human chorionic gonadotrophin priming before immature oocyte retrieval from unstimulated women with polycystic ovarian syndrome. Hum. Reprod., 15, 165–170.

Journal of the American Association for Laboratory Animal Science
Copyright 2010
by the American Association for Laboratory Animal Science

Vol 49, No 2
March 2010
Pages 160–166

Lactate and Adenosine Triphosphate in the Extender Enhance the Cryosurvival of Rat Epididymal Sperm

Hideaki Yamashiro,[1,3,*] Masaaki Toyomizu,[2] Motoi Kikusato,[2] Natsuki Toyama,[1] Satoshi Sugimura,[1] Yumi Hoshino,[1] Hiroyuki Abe,[4] Stefan Moisyadi,[3] and Eimei Sato[1]

We evaluated the cryosurvival of rat epididymal sperm preserved in raffinose–modified Krebs-Ringer bicarbonate–egg yolk extender supplemented with various energy-yielding substrates (glucose, pyruvate, lactate, and ATP) and assessed the effect on sperm oxygen consumption. The incubation of sperm at 37 °C for 10 min in lactate-free extender decreased sperm motility and oxygen consumption before and after thawing compared with those of sperm in glucose- and pyruvate-free mediums. We then focused on the effect of supplementing the extender with lactate (0, 10.79, 21.58, 32.37, and 43.16 mM) and found that sperm frozen and thawed in extender supplemented with 32.37 mM lactate exhibited the highest motility. When we supplemented extender containing 32.37 mM lactate with ATP (0, 0.92, 1.85, 3.70, and 5.55 mM), sperm frozen and thawed in the extender supplemented with 1.85 mM ATP exhibited considerably higher motility and viability than those of sperm frozen and thawed in ATP-free extender. These results provide the first evidence that supplementation of the raffinose-modified Krebs–Ringer bicarbonate–egg yolk extender with 32.37 mM lactate and 1.85 mM ATP increases of number of motile sperm before freezing and enhances the cryosurvival of rat sperm. These supplements to the extender may enhance sperm cryosurvival by improving the metabolic capacity of sperm before freezing.

Abbreviations: mKRB, modified Krebs–Ringer bicarbonate.

We previously showed that freezing rat epididymal sperm in an extender of raffinose dissolved in modified Krebs–Ringer bicarbonate (mKRB) solution containing egg yolk enhances their cryosurvival of sperm as measured by viability and acrosomal integrity; this finding suggested that a mKRB-based freezing extender containing glucose, pyruvate, and lactate can protect sperm against freezing injury.[33] A possible reason for this finding is that sperm in this extender retain high metabolic capacity before freezing which, in turn, may enhance the cryosurvival of rat sperm. However, the mechanism by which the mKRB-based extender promotes the metabolic capacity and cryosurvival of rat sperm is unclear.

The process of cryopreservation imposes numerous stresses on not only the physical features of sperm but also the energy production to support motility before and after freezing, and improving energy production in frozen–thawed sperm is important for successful cryopreservation.[19] Sugars play various roles in sperm extender solution, including providing an energy substrate for sperm during cooling and acting as a cryoprotectant.[1] The beneficial effects of adding glucose to the extender on the viability of frozen–thawed sperm have been reported for various species;[2] this nutritional effect may involve the synthesis and provision of ATP through the glycolytic pathway to provide the energy required for sperm motility. Therefore, glucose may play a key role in generating energy in motile sperm and preventing freezing damage.

The addition of an exogenous substrate (such as lactate) improved the sperm motility characteristics of cattle,[11] boars,[14,21] and rabbits.[29] A previous study[9] showed that a shuttle involving the redox couple lactate–pyruvate and lactate dehydrogenase isozyme C_4 is active in rat and rabbit mitochondria but not in mouse mitochondria. This finding suggests that sperm from various species, including rats, may find lactate a suitable substrate for maintaining the energy production and consumption as well as oxygen consumption. However, which of the major biochemical pathways—glycolysis or oxidative phosphorylation—is involved in supplying energy to mobilize sperm has been a long-lasting debate, because the pathway of energy production is species-specific.[8,28,32] Regardless of the identity of the pathway involved in energy supply, the development of an appropriate freezing extender likely would improve sperm motility and survival during cryopreservation through enhancement of the metabolic capacities of sperm. However, no previous studies have reported on the optimal components, especially the energy substrates, of a cryodiluent for the freezing of rat sperm.

Sperm may attain access to eggs by mobilizing metabolic energy production in the form of ATP to drive motility.[30] ATP is hydrolyzed by the dynein adenosine triphosphatase, which converts the chemical energy of ATP into mechanical energy used for the movement of sperm.[3,15] ATP can have several downstream effects leading to improvement in the motility of sperm by means of an increase in the calcium level.[10,17,18,20,25,27] Moreover, the amount of ATP required for metabolic energy is higher in the cytosol than the mitochondria.[16] Therefore, sup-

Received: 02 Jul 2009. Revision requested: 06 Aug 2009. Accepted: 24 Aug 2009.
[1]Laboratory of Animal Reproduction and [2]Laboratory of Animal Nutrition, Graduate School of Agricultural Science, Tohoku University, Sendai, Japan; [3]Institute for Biogenesis Research, Department of Anatomy and Reproductive Biology, John A Burns School of Medicine, University of Hawaii, Honolulu, HI; [4]Graduate School of Science and Engineering, Yamagata University, Yamagata, Japan.
**Corresponding author. Email: hideaki6@hawaii.edu*

plementation of the freezing extender with exogenous ATP may improve the cryosurvival of rat epididymal sperm.

Here we evaluated the cryosurvival and parameters of mitochondrial activity, including oxygen consumption, of rat sperm diluted in raffinose–mKRB–egg yolk extender supplemented with various energy-yielding substrates, including glucose, pyruvate, lactate, and ATP. In addition, we identified the optimal energy substrates and other components of a cryodiluent for the freezing of rat sperm.

Materials and Methods

Principles of laboratory animal care were followed during this study, and all procedures were conducted in accordance with guidelines of the Ethics Committee for Care and Use of Laboratory Animals for Research of the Graduate School of Agricultural Science (Tohoku University, Japan). Wistar rats were used throughout the experiments. Animals were kept in polycarbonate cages (25 × 40 × 20 cm) under controlled conditions with lights on at 0800 and off at 2000. They were given food and tap water ad libitum.

Preparation of the raffinose–mKRB–egg yolk extender. The basic extender used in this study was the raffinose–mKRB–egg yolk freezing solution defined previously;[33] it comprised 0.1 M raffinose (Sigma, St Louis, MO), 94.6 mM NaCl (Wako Pure Chemical Industries, Osaka, Japan), 4.78 mM KCl (Wako), 1.71 mM $CaCl_2 \cdot 2H_2O$ (Wako), 1.19 mM $MgSO_4 \cdot 7H_2O$ (Wako) 1.19 mM KH_2PO_4 (Wako), 25.07 mM $NaHCO_3$ (Wako), 21.58 mM sodium DL-lactate (Sigma), 0.5 mM sodium pyruvate (Wako), 5.56 mM glucose (Wako), 50 μg/mL streptomycin (Sigma), and 75 μg/mL penicillin (Sigma); egg yolk was separated from the albumin, and 20% (v:v) egg yolk was added to the raffinose–mKRB solution. Egg yolk lipids were solubilized by adding 0.04% (w:v) SDS (Wako) to the solution. The solution was centrifuged twice at 7000 × *g* for 30 min. The pH of the solution was adjusted to 7.3 with HCl and its osmotic pressure to 400 mOsm. The supernatant was aspirated and filtered through a 0.45-μm membrane filter (Sartorius, Goettingen, Germany).

Evaluation of sperm motility parameters. Sperm motility parameters were assessed by using a sperm motility analysis system (version 1.0, Kashimura, Tokyo, Japan) and a 10-μm deep Makler chamber (Sefi Medical Instruments, Haifa, Israel); the protocol was described previously.[6] At least 100 sperm and 5 fields were assessed by the sperm motility analysis system for each treatment group. The following parameters were assessed in this study: motility (%), straight line velocity (μm/s), curvilinear velocity (μm/s), amplitude of lateral head displacement (μm), and beat cross frequency (Hz).

Evaluation of sperm acrosome integrity. The acrosomal integrity of fresh and frozen–thawed sperm was assessed by staining with FITC-conjugated peanut agglutinin (Wako) according to the procedure described previously.[33]

Collection of rat epididymal sperm. Both caudae epididymides were excised from 24 sexually mature male Wistar rats older than 15 wk. The excised epididymis was rinsed and carefully blotted free of blood and adipose tissues. A small part of the caudae epididymides tract was excised with fine scissors. The droplet of sperm that welled up was transferred to a 1.5-mL microfuge tube containing 1 mL of freezing medium at 37 °C. After 5 min, the solution was examined macroscopically to verify that sperm were dispersed adequately.

Cryopreservation and thawing. ***Experiment 1a.*** In this experiment, we investigated the effect of the substrates glucose, pyruvate, and lactate in raffinose–mKRB–egg yolk freezing extender on the motility characteristics of fresh sperm after collection and frozen–thawed sperm. Sperm from both the caudae epididymides from 3 rats were used in this experiment. Immediately after collection, aliquots of sperm were exposed to the following 5 solutions: raffinose–mKRB–egg yolk extender containing the substrates glucose, pyruvate, and lactate (control); glucose-free extender; pyruvate-free extender; lactate-free extender; and substrate-free extender. The osmotic pressure of these solutions was adjusted to 400 mOsm with sucrose (Wako) and the pH to 7.3 with HCl. Each sperm suspension was incubated at 37 °C for 5 min to allow the sperm to disperse, and the sperm concentration and motility parameters then were evaluated by the sperm motility analysis system. The sperm were processed and frozen by using a modification of a previously published protocol.[33] The diluted sperm samples were cooled at 5 °C for 90 min. The sperm samples were further diluted 1:1 with each extender containing 1.5% of a commercial cryoprotectant (Equex STM, Nova Chemical Sales, Scituate, MA) to obtain a sperm concentration of 5×10^6 sperm/mL and then were equilibrated at 5 °C for 30 min before freezing. Afterward, the samples were loaded into standard 0.5-mL straws and the straws were heat-sealed. The straws were placed in liquid nitrogen vapor for 10 min, plunged into liquid nitrogen (–196 °C), and stored for 3 d at this temperature. The straws were thawed rapidly by holding them in water (37 °C) for 10 s. The sperm were transferred to a 1.5-mL microfuge tube and incubated at 37 °C for 5 min, after which motility parameters after thawing were assessed by using the sperm motility analysis system. The acrosome status of frozen–thawed sperm was assessed by staining with FITC-conjugated peanut agglutinin.[1]

Experiment 1b. Building on the results of Experiment 1a, this experiment was conducted to analyze the characteristics of fresh and frozen–thawed sperm in the raffinose–mKRB–egg yolk extender containing various concentrations of lactate. Sperm from both caudae epididymides from 3 rats were used. Aliquots of sperm were suspended in 1 mL raffinose–mKRB–egg yolk extender containing 0, 10.79, 21.58, 32.37, or 43.16 mM lactate; all of these solutions had an osmotic pressure of 400 mOsm and a pH of 7.3, except the solution containing 43.16 mM lactate (430 mOsm and pH 7.3). The procedures followed for cryopreservation and evaluation of sperm were the same as described for experiment 1a.

Experiment 1c. This experiment was designed to compare the cryosurvival of rat sperm frozen in raffinose–mKRB–egg yolk extender solution containing 32.37 mM lactate supplemented with various concentrations of ATP. Both caudae epididymides from 3 male rats were used in this experiment. After collection, sperm was divided into 5 aliquots and suspended in 1 mL of extender solution containing 32.37 mM lactate and 0, 0.92, 1.85, 3.70, or 5.55 mM ATP (400 mOsm and pH 7.3). The freezing protocol and evaluation of sperm were the same as described previously. For the evaluation of sperm viability, frozen–thawed sperm samples were incubated in a water bath at 37 °C for 5 min. For each treatment, 3 samples were evaluated after 1, 2, and 3 h of incubation to determine sperm motility, straight-line velocity, curvilinear velocity, and amplitude of lateral head displacement.

Measurement of oxygen consumption of sperm. ***Experiment 2a.*** The aim of this experiment was to assess the effect of substrates in the raffinose–mKRB–egg yolk medium on the mitochondrial activity of sperm. Sperm was collected from 5 mature male rats and extended in substrate-free raffinose–mKRB–egg yolk medium at 37 °C. The sample was incubated for 5 min to allow the sperm to disperse and then equal volumes were resuspended in each of the following solutions: raffinose–

mKRB–egg yolk medium containing 11.12 mM glucose, 1 mM pyruvate, and 43.16 mM lactate (control); glucose-free control (containing pyruvate and lactate); pyruvate-free control (containing glucose and lactate); lactate-free control (containing glucose and pyruvate); and substrate-free raffinose–mKRB–egg yolk medium. The final concentrations of the various substrates in medium containing sperm were 5.56 mM glucose, 0.5 mM pyruvate, and 21.58 mM lactate. The osmotic pressure of these solutions was adjusted to 400 mOsm with sucrose and the pH to 7.3 with HCl. The oxygen consumption rates of the sperm were measured by using Clark-type oxygen electrodes (Rank Brothers, Cambridge, UK) maintained at 37 °C for 10 min and calibrated with air-saturated water at 37 °C, which was assumed to contain 406 nmol oxygen/mL.[26] A sperm sample in a volume of 1 mL was suspended in the reaction chamber by stirring carefully to prevent the addition of any external air. The final concentration of sperm in the incubation chamber was approximately 1×10^7 sperm/mL. Data were acquired by using a commercial software program (LabChart version 5.2, AD Instruments, Castle Hill, Australia). The oxygen consumed by the sperm was calculated as:[26]

> Oxygen concentration (nmol oxygen/mL) = oxygen (U) × oxygen concentration of air-saturated water (that is, 406 nmol oxygen/mL) ÷ oxygen full-chart span (U)

The rate of oxygen consumption by sperm was expressed as nmol/min/1×10^7 sperm.

Experiment 2b. The effect of various concentrations of lactate in the raffinose–mKRB–egg yolk extender on the oxygen uptake of sperm was analyzed. Sperm were collected from the caudae epididymides of 5 rats and suspended in lactate-free raffinose–mKRB–egg yolk medium and then incubated for 5 min at 37 °C. Equal volumes of raffinose–mKRB–egg yolk medium containing 0, 21.58, 43.16, 64.74, and 86.32 mM lactate were diluted with lactate-free raffinose–mKRB–egg yolk medium, resulting in solutions with final lactate concentrations of 0, 10.79, 21.58, 32.37, and 43.16 mM, respectively. The osmotic pressure and the pH of all these solutions were adjusted to 400 mOsm and 7.3, respectively, except the solution containing 43.16 mM lactate (430 mOsm and pH 7.3). The oxygen consumption of each sperm suspension was determined in relation to air-saturated medium as described for experiment 2b.

Experiment 2c. The effect of adding ATP to raffinose–mKRB–egg yolk medium containing 32.37 mM lactate on the rate of oxygen consumption of sperm was examined. Sperm from 5 rats were flushed the sperm out by using the medium, and then the suspensions in ATP-free raffinose–mKRB–egg yolk medium were incubated for 5 min at 37 °C. Each treated sample was placed in raffinose–mKRB–egg yolk medium containing 0, 1.84, 3.70, 7.4, or 11.1 mM ATP. Subsequently, equal volumes of extended sperm were added to these solutions, resulting in solutions with final ATP concentrations of 0, 0.92, 1.85, 3.70, and 5.55 mM (400 mOsm and pH 7.3). The oxygen consumption of the sperm was determined as described for experiment 2a.

Statistical analysis. The data were subjected to ANOVA and the Fisher protected least-significant difference post hoc test (StatView, Abacus Concepts, Berkeley, CA). All data are expressed as mean ± SEM. A P value of less than 0.05 indicated statistical significance.

Results

Effect of various substrates in raffinose–mKRB–egg yolk extender on fresh and frozen–thawed sperm (experiment 1a). The first experiment in this series was aimed at assessing the effect of various energy-yielding substrates in the raffinose–mKRB–egg yolk extender on the motility characteristics of fresh and frozen–thawed sperm. The motility of sperm added to the medium without the substrates glucose, pyruvate, and lactate was significantly ($P < 0.05$) lower than that of sperm added to the medium containing all 3 of these substrates (control; Table 1); this result was obtained from both fresh and frozen–thawed sperm. In contrast, the sperm motility and motion parameters did not differ significantly between fresh and frozen–thawed sperm when glucose-free and pyruvate-free solutions were used. The medium that contained glucose, pyruvate, and lactate resulted in the highest motility of frozen–thawed sperm. The percentage of intact acrosomes did not differ significantly among sperm treated with the various extenders for both fresh and frozen–thawed sperm (Table 1).

Effect of lactate in raffinose–mKRB–egg yolk extender on fresh and frozen–thawed sperm (experiment 1b). According to the results of experiment 1a, lactate was the most effective agent for increasing the motility of both fresh and frozen–thawed sperm. We therefore investigated the effect of adding lactate at 0, 10.79, 21.58, 32.37, and 43.16 mM to the raffinose–mKRB–egg yolk medium on the motility of sperm. Sperm diluted in lactate-free extender showed significantly ($P < 0.05$) lower motility than did sperm diluted in extender containing 21.58 or 32.37 mM lactate (Table 2). The data revealed that sperm frozen in the raffinose–mKRB–egg yolk extender containing 32.37 mM lactate showed significantly ($P < 0.05$) higher motility after thawing than did sperm frozen in substrate-free extender. The proportion of sperm with intact acrosomes either before or after thawing did not differ significantly among extenders containing 0, 10.79, 21.58, 32.37, or 43.16 mM lactate.

Effect of ATP in raffinose–mKRB–egg yolk extender containing 32.37 mM lactate on fresh and frozen–thawed sperm (experiment 1c). The effect of adding 0, 0.92, 1.85, 3.70, or 5.55 mM ATP to raffinose–mKRB–egg yolk extender containing 32.37 mM lactate on the cryosurvival of the sperm are summarized in Table 3. Sperm frozen in extender containing 32.37 mM lactate and 1.85 mM ATP exhibited significantly ($P < 0.05$) higher motility than that of sperm frozen in ATP-free extender. The sperm frozen and thawed in extender supplemented with 1.85 mM ATP maintained significantly ($P < 0.05$) higher motility throughout the 3-h incubation at 37 °C than did sperm frozen and thawed in the ATP-free extender (Figure 1). The addition of ATP to the extender increased the proportion of intact acrosomes in after collected sperm, and among all concentrations of ATP tested, the percentage of intact acrosomes was highest at 1.85 mM ATP. Similar results were obtained for the acrosome status of frozen–thawed sperm.

Effect of glucose, pyruvate, and lactate in raffinose–mKRB–egg yolk medium on the oxygen consumption of sperm (experiment 2a). In the next series of experiments, we examined the effect of the substrates glucose, pyruvate, and lactate in the raffinose–mKRB–egg yolk medium on the rate of oxygen consumption of sperm. Incubation of the sperm suspension with lactate-free medium resulted in a significant ($P < 0.05$) decline in the rate of oxygen consumption during incubation as compared with the incubation of the sperm suspension with medium containing glucose, pyruvate, and lactate (Figure 2). The oxygen consumption of sperm in medium lacking any added substrates tended to be decreased compared with that of sperm in the complete

Table 1. Effect of the substrates glucose, pyruvate, and lactate in raffinose–mKRB–egg yolk extender on fresh and frozen–thawed sperm

	Sperm characteristics	Control	–Glucose	–Pyruvate	–Lactate	Substrate-free
Fresh sperm	Motility (%)	78.2 ± 8.0	70.8 ± 2.6	67.3 ± 8.0	54.9 ± 6.1	44.8 ± 3.9[a]
	VSL (μm/s)	17.4 ± 1.2	16.5 ± 3.3	10.9 ± 1.4	15.4 ± 1.0	11.1 ± 1.9
	VCL (μm/s)	124.2 ± 3.1	115.1 ± 8.6	109.8 ± 1.9	108.3 ± 2.9	102.4 ± 4.1
	ALD (μm)	6.9 ± 0.1	6.5 ± 0.5	6.5 ± 0.2	6.5 ± 0.1	5.8 ± 0.3
	BCF (Hz)	22.2 ± 0.8	23.3 ± 1.8	25.4 ± 1.6	23.4 ± 1.0	29.0 ± 0.6
	Acrosomal integrity (%)	84.5 ± 2.9	76.2 ± 1.9	79.6 ± 4.9	77.1 ± 2.4	81.4 ± 4.4
Frozen–thawed sperm	Motility (%)	21.5 ± 1.4	23.2 ± 0.9	19.8 ± 1.3	13.8 ± 2.4[a]	13.7 ± 1.5[a]
	VSL (μm/s)	3.9 ± 0.4	3.2 ± 0.5	3.9 ± 0.4	3.9 ± 0.3	4.4 ± 0.8
	VCL (μm/s)	85.4 ± 8.7	71.8 ± 4.7	89.2 ± 13.2	77.8 ± 5.5	69.3 ± 7.4
	ALD (μm)	4.2 ± 0.5	3.3 ± 0.2	4.1 ± 0.5	3.8 ± 0.2	3.2 ± 0.5
	BCF (Hz)	32.2 ± 3.7	31.3 ± 1.6	36.2 ± 1.8	34.1 ± 0.9	31.7 ± 2.5
	Acrosomal integrity (%)	68.1 ± 4.0	71.3 ± 5.8	70.0 ± 2.0	64.1 ± 5.3	70.6 ± 2.3

ALD, amplitude of lateral head displacement; BCF, beat cross frequency; VCL, curvilinear velocity; VSL, straight-line velocity.
Data are presented as mean ± SEM (n = 3).
[a]Value significantly ($P < 0.05$) different from control value.

Table 2. Effect of lactate in raffinose–mKRB–egg yolk extender on fresh and frozen–thawed sperm

		Lactate concentration (mM)				
	Sperm characteristics	0	10.79	21.58	32.37	43.16
Fresh sperm	Motility (%)	47.4 ± 4.9	46.3 ± 13.2	61.3 ± 2.1	67.5 ± 3.8[a]	55.1 ± 3.7
	VSL (μm/s)	12.5 ± 1.7	8.8 ± 1.0	16.5 ± 2.6	12.3 ± 1.2	9.8 ± 3.0
	VCL (μm/s)	98.3 ± 6.3	86.0 ± 2.7	94.6 ± 10.0	92.9 ± 3.1	95.9 ± 6.5
	ALD (μm)	5.3 ± 0.4	5.3 ± 0.3	4.8 ± 0.6	4.7 ± 0.3	5.1 ± 0.3
	BCF (Hz)	26.4 ± 1.4	24.7 ± 1.3	22.5 ± 0.8	24.5 ± 0.8	25.6 ± 1.3
	Acrosomal integrity (%)	75.9 ± 0.5	71.7 ± 4.0	73.6 ± 5.9	75.1 ± 0.5	71.8 ± 1.8
Frozen–thawed sperm	Motility (%)	11.3 ± 2.2	17.5 ± 3.5	19.7 ± 2.8	22.3 ± 4.0[a]	12.6 ± 4.3
	VSL (μm/s)	3.5 ± 0.6	2.8 ± 0.3	3.6 ± 0.2	3.8 ± 0.1	4.9 ± 0.5
	VCL (μm/s)	78.6 ± 8.2	75.0 ± 3.5	78.5 ± 4.2	95.0 ± 14.1	126.9 ± 5.1[a]
	ALD (μm)	3.4 ± 0.6	3.3 ± 0.1	3.5 ± 0.2	4.5 ± 0.6	5.5 ± 0.4[a]
	BCF (Hz)	44.8 ± 1.5	36.7 ± 1.8	39.8 ± 0.8	36.5 ± 2.3	42.9 ± 2.1
	Acrosomal integrity (%)	69.3 ± 2.9	71.6 ± 0.4	69.0 ± 0.2	69.2 ± 0.2	61.5 ± 1.8

ALD, amplitude of lateral head displacement; BCF, beat cross frequency; VCL, curvilinear velocity; VSL, straight-line velocity.
Data are presented as mean ± SEM (n = 3).
[a]Value significantly ($P < 0.05$) different from control value.

medium. In contrast, oxygen consumption did not differ significantly between sperm in glucose- or pyruvate-free media and those in the medium containing glucose, pyruvate, and lactate.

Effect of lactate in raffinose–mKRB–egg yolk medium on the oxygen consumption of sperm (experiment 2b). The respiration capacity of sperm was tested after their incubation in a lactate-free raffinose–mKRB–egg yolk medium or in a medium supplemented with 10.79, 21.58, 32.37, or 43.16 mM lactate (Figure 3). Oxygen uptake was significantly ($P < 0.05$) higher in sperm incubated in medium containing 32.37 mM lactate than in sperm incubated in lactate-free medium.

Effect of ATP in the raffinose–mKRB–egg yolk extender containing 32.37 mM lactate on the oxygen consumption of sperm (experiment 2c). This experiment evaluated the influence of supplementation of the raffinose–mKRB–egg yolk medium containing 32.37 mM lactate with various concentrations of ATP (0, 0.92, 1.85, 3.70, and 5.55 mM) on the oxygen consumption of sperm during incubation at 37 °C for 10 min (Figure 4). When the medium was supplemented with 1.85 mM ATP, the rate of oxygen consumption tended to be increased compared with that in ATP-free medium, but difference is not significant.

Discussion

The present study demonstrated that an extender of raffinose–mKRB–egg yolk containing 32.37 mM lactate enhanced the metabolic capacity and survival of rat sperm after cryopreservation. The cryosurvival of rat sperm was further improved by the addition of 1.85 mM exogenous ATP to the freezing extender.

When the oxidizable substrate lactate was not added to the raffinose–mKRB–egg yolk extender, the motility, viability, and rate of oxygen consumption decreased considerably in both fresh and frozen–thawed sperm. In contrast, sperm frozen and thawed in extender supplemented with 32.37 mM lactate exhibited higher motility than those frozen and thawed in lactate-free extender. This finding indicates that exogenous lactate in the freezing extender is a potent inducer that enhances the oxygen consumption of rat sperm and their motility after collection and freezing–thawing.

Table 3. Effect of ATP in raffinose–mKRB–egg yolk extender containing 32.37 mM lactate on fresh and frozen–thawed sperm

		ATP concentration (mM)				
		0	0.92	1.85	3.70	5.55
Fresh sperm	Motility (%)	74.7 ± 1.8	72.8 ± 8.1	79.2 ± 3.3	73.8 ± 6.6	55.6 ± 4.2[a]
	VSL (μm/s)	9.1 ± 1.7	10.1 ± 0.5	14.7 ± 3.3	7.9 ± 0.6	8.4 ± 1.4
	VCL (μm/s)	110.2 ± 9.9	116.9 ± 8.5	123.6 ± 5.2	101.5 ± 8.8	104.9 ± 7.9
	ALD (μm)	6.0 ± 0.1	7.6 ± 0.6	6.3 ± 0.6	6.8 ± 1.0	5.7 ± 0.4
	BCF (Hz)	29.9 ± 2.8	34.0 ± 1.7	29.7 ± 2.7	32.9 ± 2.6	31.2 ± 1.5
	Acrosomal integrity (%)	75.5 ± 6.3	78.9 ± 6.5	83.2 ± 1.6	82.5 ± 7.2	77.1 ± 7.1
Frozen–thawed sperm	Motility (%)	20.6 ± 0.3	24.6 ± 0.9	35.3 ± 1.3[a]	26.9 ± 1.4	25.7 ± 7.2
	VSL (μm/s)	6.0 ± 1.2	5.0 ± 0.2	4.1 ± 0.6	4.4 ± 0.6	3.0 ± 0.4
	VCL (μm/s)	99.0 ± 8.3	89.3 ± 4.5	84.5 ± 4.1	85.8 ± 2.7	80.9 ± 3.9
	ALD (μm)	5.2 ± 0.8	4.4 ± 0.4	4.3 ± 0.1	4.3 ± 0.1	3.4 ± 0.1
	BCF (Hz)	37.1 ± 2.0	34.4 ± 0.6	35.0 ± 1.6	34.6 ± 5.0	37.2 ± 2.2
	Acrosomal integrity (%)	67.7 ± 2.3	68.4 ± 8.8	70.6 ± 4.6	61.7 ± 3.5	66.5 ± 3.8

ALD, amplitude of lateral head displacement; BCF, beat cross frequency; VCL, curvilinear velocity; VSL, straight-line velocity.
Data are presented as mean ± SEM (n = 3).
[a]Value significantly ($P < 0.05$) different from control value.

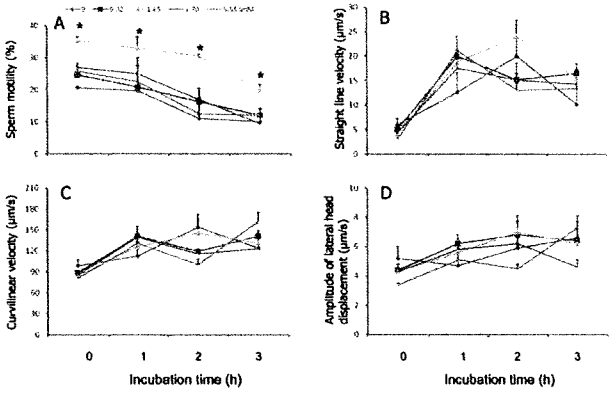

Figure 1. Effect of ATP in raffinose–mKRB–egg yolk medium containing 32.37 mM lactate on the (A) motility, (B) straight line velocity, (C) curvilinear velocity, and (D) amplitude of lateral head displacement of frozen–thawed sperm during incubation at 37 °C for 3 h. Data are presented as mean ± SEM (n = 3). *, Value significantly ($P < 0.05$) different from control value.

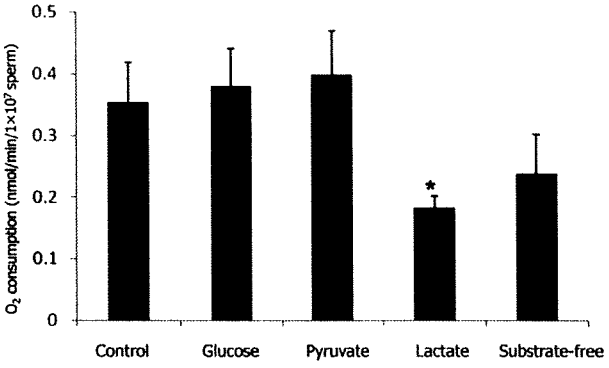

Figure 2. Effect of glucose, pyruvate, and lactate in raffinose–mKRB–egg yolk medium on the oxygen consumption of fresh sperm during incubation at 37 °C for 10 min. Data are presented as mean ± SEM (n = 5). *, Value significantly ($P < 0.05$) different from control value.

The sperm-specific enzyme lactate dehydrogenase isozyme C_4 is located in the cytosol and the matrix of the mitochondria in the midpiece of rat sperm. Further, a study[9] has revealed that both a shuttle involving the redox couple lactate–pyruvate and lactate dehydrogenase isozyme C_4 are active in rat sperm mitochondria. In another study,[12] the lactate concentration in oviductal fluids was 10-fold higher than the glucose concentration, and the lactate concentration in the uterine fluids was 15-fold higher than the glucose concentration during the murine estrous cycle. Therefore, it is very likely that lactate is used by rat sperm as an essential substrate to maintain highly regulated ATP production and dissipation: lactate in the cytosol and mitochondrial matrix is oxidized to pyruvate by mitochondrial lactate dehydrogenase isozyme C_4, and pyruvate is oxidized through the Krebs cycle and electron transport chain.[4,5,23,24] To our knowledge, our findings are the first evidence showing that rat sperm can use exogenous lactate in the cryodiluent as an essential substrate to maintain highly regulated metabolic capacity and that this lactate acts as an energy substrate for mitochondria to the mobilization of fresh and frozen–thawed sperm.

Mitochondria, the site of ATP generation due to oxidative phosphorylation, are localized solely in the midpiece of sperm.[22] The oxidative production of ATP through the Krebs cycle is an essential function of the midpiece mitochondria for motility.[31] The mitochondrial biochemical pathways of oxidative phosphorylation are 15 times more efficient than is anaerobic glycolysis for ATP production.[7,28] These findings also support our arguments that the energy production and dissipation in rat sperm are highly dependent on the mitochondria.

The present study showed that supplementation of raffinose–mKRB–egg yolk extender with 32.37 mM lactate and 1.85 mM exogenous ATP considerably increases sperm motility before freezing, thus improving the survivability of sperm after cryopreservation. Exogenous ATP in the freezing medium may be responsible for the generation of multiple metabolic signals that appear to be related to the sperm motility through a rise in calcium levels;[10,17,18,20,25,27] this reaction increases de novo ATP synthesis before freezing and may contribute to the remobilization of sperm after freezing–thawing. The motility of ram sperm was restored by exogenous ATP that crossed plasma membrane when the membrane was damaged by cryopreservation.[13] In light of that finding,[13] we cannot discount that our result is caused by the facultative transport of ATP across plasma membrane because of damage during freezing, thereby allow-

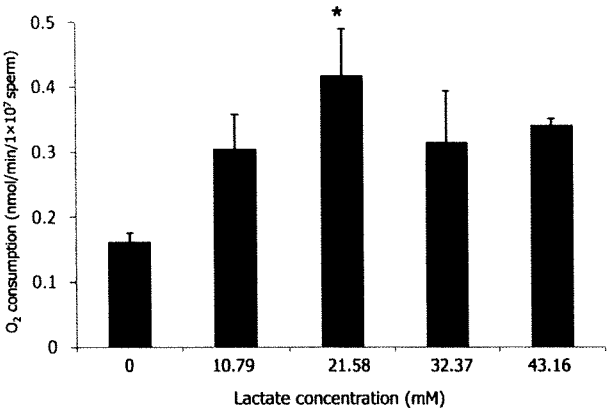

Figure 3. Effect of lactate in raffinose–mKRB–egg yolk medium on oxygen consumption of fresh sperm during incubation at 37 °C for 10 min. Data are presented as mean ± SEM (n = 5). *, Value significantly ($P < 0.05$) different from control value.

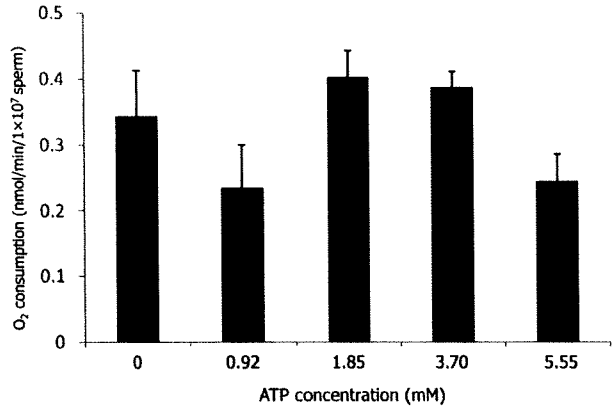

Figure 4. Effect of ATP in raffinose–mKRB–egg yolk medium containing 32.37 mM lactate on oxygen consumption of fresh sperm during incubation at 37 °C for 10 min. Data are presented as mean ± SEM (n = 5). *, Value significantly ($P < 0.05$) different from control value.

ing substrates to directly access ATP and allowing adenosine triphosphatase to use ATP directly to generate energy for the mobilization of rat sperm.

In conclusion, the current study demonstrated that the addition of lactate and ATP to the raffinose–mKRB–egg yolk extender before freezing increases the number of motile sperm and mediates the energy-dependent synthetic processes of rat epididymal sperm. In turn, these effects may increase the cryosurvival of rat sperm. Further investigation of species-specific differences in the energy-dependent synthetic processes in sperm may prove valuable in defining the ideal components of a cryodiluent, which interact to regulate the cryosurvival of rat sperm, and in clarifying the adaptations needed for cryopreservation of sperm from other species.

Acknowledgment

This work was supported in part by grants 19658102 and 16108003 (to ES) from the Japan Society for the Promotion of Science.

References

1. **Aboagla EM, Terada T.** 2003. Trehalose enhanced fluidity of the goat sperm membrane and its protection during freezing. Biol Reprod **69:**1245–1250.
2. **Barbas JP, Mascarenhas RD.** 2009. Cryopreservation of domestic animal sperm cells. Cell Tissue Bank **10:**49–62.
3. **Brokaw CJ.** 1972. Flagellar movement: a sliding filament model. Science **178:**455–462.
4. **Brooks GA, Dubouchaud H, Brown M, Sicurello JP, Butz CE.** 1999. Role of mitochondrial lactate dehydrogenase and lactate oxidation in the intracellular lactate shuttle. Proc Natl Acad Sci USA **96:**1129–1134.
5. **Brooks GA.** 2002. Lactate shuttles in nature. Biochem Soc Trans **30:**258–264.
6. **Cancel AM, Lobdell D, Mendola PP, Perreault SD.** 2000. Objective evaluation of hyperactivated motility in rat spermatozoa using computer-assisted sperm analysis. Hum Reprod **15:**1322–1328.
7. **Cardullo RA, Baltz JM.** 1991. Metabolic regulation in mammalian sperm: mitochondrial volume determines sperm length and flagellar beat frequency. Cell Motil Cytoskeleton **19:**180–188.
8. **Ford WCL.** 2006. Glycolysis and sperm motility: does a spoonful of sugar help the flagellum go round? Hum Reprod Update **12:**269–274.
9. **Gallina FG, Deburgos NMG, Burgos C, Coronel CE, Blanco A.** 1994. The lactate–pyruvate shuttle in spermatozoa: operation in vitro. Arch Biochem Biophys **308:**515–519.
10. **Gibbons IR.** 1963. Studies on the protein components of cilia from *Tetrahymena pyriformis*. Proc Natl Acad Sci USA **50:**1002–1010.
11. **Halang KW, Bohnensack R, Kunz W.** 1985. Interdependence of mitochondrial ATP production and extramitochondrial ATP utilization in intact spermatozoa. Biochim Biophys Acta **808:**316–322.
12. **Harris SE, Gopichandran N, Picton HM, Leese HJ, Orsi NM.** 2005. Nutrient concentrations in murine follicular fluid and the female reproductive tract. Theriogenology **64:**992–1006.
13. **Holt WV, Head MF, North RD.** 1992. Freeze-induced membrane damage in ram spermatozoa is manifested after thawing: observations with experimental cryomicroscopy. Biol Reprod **46:**1086–1094.
14. **Jones AR.** 1997. Metabolism of lactate by mature boar spermatozoa. Reprod Fertil Dev **9:**227–232.
15. **Kamp G, Busselmann G, Lauterwein J.** 1996. Spermatozoa: models for studying regulatory aspects of energy metabolism. Experientia **52:**487–494.
16. **Klingenberg M.** 1979. The ADP–ATP shuttle of the mitochondrion. Trends Biochem Sci **4:**249–252.
17. **Kinukawa M, Oda S, Shirakura Y, Okabe M, Ohmuro J, Baba SA, Nagata M, Aoki F.** 2006. Roles of cAMP in regulating microtubule sliding and flagellar bending in demembranated hamster spermatozoa. FEBS Lett **580:**1515–1520.
18. **Litvin TN, Kamenetsky M, Zarifyan A, Buck J, Levin LR.** 2003. Kinetic properties of 'soluble' adenylyl cyclase: synergism between calcium and bicarbonate. J Biol Chem **278:**15922–15926.
19. **Long JA.** 2006. Avian semen cryopreservation: what are the biological challenges? Poult Sci **85:**232–236.
20. **Luria A, Rubinstein S, Lax Y, Breitbart H.** 2002. Extracellular adenosine triphosphate stimulates acrosomal exocytosis in bovine spermatozoa via P2 purinoceptor. Biol Reprod **66:**429–437.
21. **Medrano A, Fernández-Novell JM, Ramió L, Alvarez J, Goldberg E, Rivera MM, Guinovart JJ, Rigau T, Rodríguez-Gil JE.** 2006. Utilization of citrate and lactate through a lactate-dehydrogenase- and ATP-regulated pathway in boar spermatozoa. Mol Reprod Dev **73:**369–378.
22. **Millette CF, Spear PG, Gall WE, Edelman GM.** 1973. Chemical dissection of mammalian spermatozoa. J Cell Biol **58:**662–675.
23. **Montamat EE, Vermouth NT, Blanco A.** 1988. Subcellular localization of branched-chain amino acid aminotransferase and lactate dehydrogenase C4 in rat and mouse spermatozoa. Biochem J **255:**1053–1056.
24. **Poole RC, Halestrap AP.** 1993. Transport of lactate and other monocarboxylates across mammalian plasma membranes. Am J Physiol **264(4Pt 1):**C761–C782.
25. **Ren D, Navarro B, Perez G, Jackson AC, Hsu SQ, Shi Q, Tilly JL, Clapham DE.** 2001. A sperm ion channel required for sperm motility and male fertility. Nature **413:**603–609.

26. **Reynafarje B, Costa LE, Lehninger AL.** 1985. O_2 solubility in aqueous media determined by a kinetic method. Anal Biochem **145:**406–418.
27. **Rodriguez-Miranda E, Buffone MG, Edwards SE, Ord TS, Lin K, Sammel MD, Gerton GL, Moss SB, William CJ.** 2008. Extracellular adenosine 5′-triphosphate alters motility and improves the fertilizing capability of mouse sperm. Biol Reprod **79:**164–171.
28. **Ruiz-Pesini E, Díez-Sánchez C, López-Pérez MJ, Enríquez JA.** 2007. The role of the mitochondrion in sperm function: is there a place for oxidative phosphorylation or is this a purely glycolytic process? Curr Top Dev Biol **77:**3–19.
29. **Storey BT, Kayne FJ.** 1978. Energy metabolism of spermatozoa. VII. Interactions between lactate, pyruvate and malate as oxidative substrates for rabbit sperm mitochondria. Biol Reprod **18:**527–536.
30. **Storey BT.** 2008. Mammalian sperm metabolism: oxygen and sugar, friend and foe. Int J Dev Biol **52:**427–437.
31. **Suarez SS, Marquez B, Harris TP, Schimenti JC.** 2007. Different regulatory systems operate in the midpiece and principal piece of the mammalian sperm flagellum. Soc Reprod Fertil Suppl **65:**331–334.
32. **Turner RM.** 2003. Tales from the tail: what do we really know about sperm motility? J Androl **24:**790–803.
33. **Yamashiro H, Han YJ, Sugawara A, Tomioka I, Hoshino Y, Sato E.** 2007. Freezability of rat epididymal sperm induced by raffinose in modified Krebs–Ringer bicarbonate (mKRB) based extender solution. Cryobiology **55:**285–294.

CASE REPORT

A birth from the transfer of a single vitrified-warmed blastocyst using intracytoplasmic sperm injection with calcium ionophore oocyte activation in a globozoospermic patient

Koichi Kyono, M.D.,[a] *Yukiko Nakajo, B.S.,*[a] *Chikako Nishinaka, B.S.,*[a] *Hiromitsu Hattori, B.S.,*[a] *Toshihiko Kyoya, B.S.,*[a] *Takayuki Ishikawa, Ph.D.,*[a] *Hiroyuki Abe, Ph.D.,*[b] *and Yasuhisa Araki, Ph.D.*[c]

[a] Kyono ART Clinic, Mitsui-Seimei, Honcho, Aobaku, Sendai; [b] Graduate School of Science and Engineering, Yamagata University, Jyounan, Yonezawa, Yamagata; and [c] Institute for ARMT, Ishii, Fujimi, Setagun, Gunma, Japan

Objective: To present the effectiveness of diagnostic heterologous intracytoplasmic sperm injection (ICSI), mouse oocyte activation test (MOAT), and ICSI combined with assisted oocyte activation (AOA) in a globozoospermic patient.
Design: A case report.
Setting: A private IVF center, Japan.
Patient(s): A patient with globozoospermia.
Intervention(s): MOAT in a mouse and ICSI combined with AOA in a human.
Main Outcome Measure(s): Ultrastructure, MOAT, fertilization, and pregnancy.
Result(s): The transmission electron micrographs showed 100% round-headed spermatozoa lacking an acrosome. MOAT showed that the fertilization rate was 68.4% (13/19) when AOA was used but 0% (0/19) when AOA was not used. After the diagnosis of globozoospermia and sperm-related activation deficiency, 17 human mature oocytes were activated with calcium ionophore after ICSI was performed. The fertilization rate was 88.2% (15/17), and 11 blastocysts were cryopreserved using the vitrification method to prevent severe ovarian hyperstimulation syndrome. A single vitrified-warmed blastocyst was transferred. A gestational sac with fetal heart movements was recognized, and a healthy boy weighing 3180 g was born at 40 weeks of gestation by cesarean section without any congenital abnormality.
Conclusion(s): MOAT allows discrimination between sperm- and oocyte-related fertilization failures and shows the effectiveness of AOA. (Fertil Steril® 2009;91:931.e7–e11. ©2009 by American Society for Reproductive Medicine.)

Key Words: Globozoospermia, calcium ionophore A23187, strontium chloride ($SrCl_2$), ICSI, diagnostic heterologous ICSI, assisted oocyte activation (AOA), round-headed spermatozoa, lack of an acrosome

Globozoospermia is a rare (incidence <0.1% in male infertile patients) form of teratozospermia, mainly characterized by round-headed spermatozoa that lack an acrosome. It originates from a disturbed spermiogenesis, which is known to be genetic. These sperm lack acrosomal membranes and acrosin contents, so they are unable either to penetrate the zona pellucida of an oocyte or to fuse with the oolemma in vivo or in vitro. However, intracytoplasmic sperm injection (ICSI) has opened up new possibilities to couples with male factor infertility caused by globozoospermia (1–9). However, ICSI with globozoospermic cells is generally less successful compared with typical ICSI (10). Rybouchkin et al. (11) discovered that fertilization was improved when a calcium ionophore was used as well. They suggested that the sperm-associated oocyte-activating factor that normally causes the Ca^{2+} flux required for fertilization might be absent or down-regulated in globozoospermic sperm. We report a successful case of pregnancy and delivery from a transfer of a single vitrified-warmed blastocyst after performing ICSI and assisted oocyte activation (AOA) in a patient with globozoospermia and asthenozoospermia.

Received July 29, 2008; revised September 27, 2008; accepted October 3, 2008.
K.K. has nothing to disclose. Y.N. has nothing to disclose. C.N. has nothing to disclose. H.H. has nothing to disclose. T.K. has nothing to disclose. T.I. has nothing to disclose. H.A. has nothing to disclose. Y.A.
Reprint requests: Dr. Kolchi Kyono, Kyono ART Clinic, Mitsui-Seimei, Sendai Honcho Bld, 3F, 1-1-1, Honcho, Aobaku, Sendai 980-0014, Japan (FAX: 81-22-722-8840; E-mail: info@ivf-kyono.or.jp).

CASE REPORT

Informed consent was obtained from the couple before the study. The couple, with primary infertility of 2 years' duration, was healthy and had no physical issues except for the

FIGURE 1

Round-headed sperm morphology in a globozoospermic patient. (**A**) Normal sperm morphology, control aspects by light microscope. (**B**) Round-headed sperm morphology of a patient by light microscope. (**C**) Round-headed sperm morphology of a patient by electron microscope.

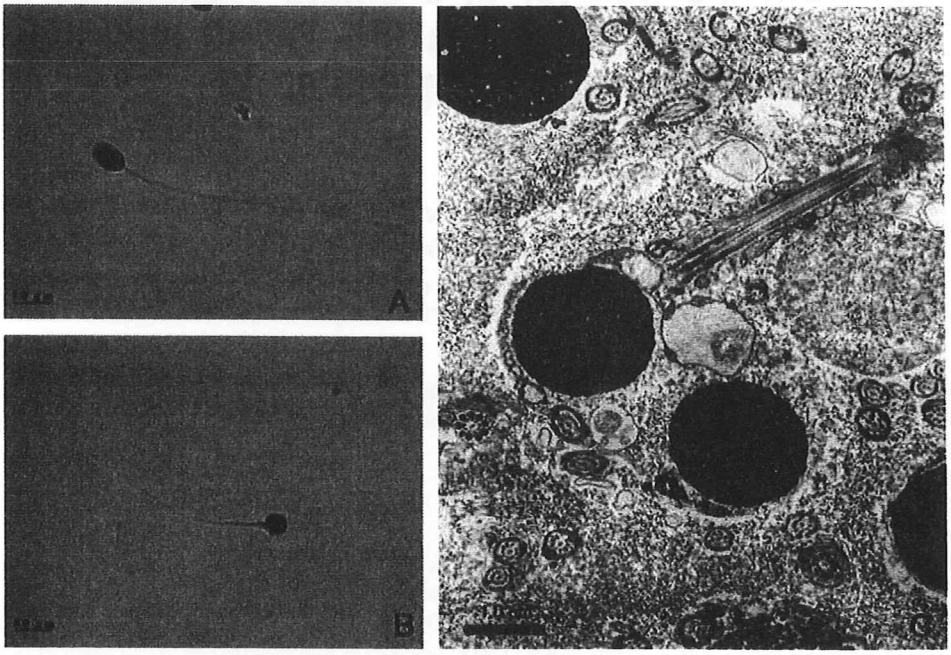

Kyono. Birth from a globozoospermic patient. Fertil Steril 2009.

husband's semen characteristics. A Kruger test showed 100% round-headed sperm with abnormal morphology. We diagnosed the husband as having globozoospermia by electron microscopy. Since we confirmed the efficacy of AOA by mouse oocyte activation test (MOAT), ICSI with AOA was performed for human oocytes.

MATERIALS AND METHODS

Patient History (Anamnesis)

Before this study, we obtained informed consent from the couple and approval from the Institutional Review Board for this study. A 29-year-old woman and her 30-year-old husband presented with primary infertility of 2 years' duration. The couple was healthy and had no physical issues except for the husband's semen aspects. The fertility of the wife was completely normal. Semen analysis showed normal values in volume (2.0 mL), concentration (38 $\times$ 10^6/mL), and motility (39%), which proved asthenozoospermia, and the analysis also showed 100% round-headed sperm with abnormal morphology on light and electron microscopy (Fig. 1). The karyotypes of the couple were 46,XX (wife) and 46,XY (husband) on peripheral lymphocytes.

Fixation and Observation for Electron Microscopy

Sperm were processed for transmission electron microscopy using the method described elsewhere (12), by which they were collected with centrifugation and fixed in chilled 2.5% glutaraldehyde (Wako; Osaka, Japan) solution in 0.1 M phosphate buffer, pH 7.4. After they were washed with chilled 0.1 M phosphate buffer, the sperm were postfixed in chilled 1% osmium teroxide (Taab Laboratories Equipment Ltd., Berkshire, UK) in 0.1 M phosphate buffer, dehydrated in a series of graded ethanol, and embedded in epoxy resin (Taab Laboratories Equipment Ltd.). Ultrathin sections were cut with a diamond knife using an ultramicrotome (Reichert Ultracuts, Leica; Heerbrugg, Switzerland), stained with uranyl acetate and lead citrate, and examined by a transmission electron microscope (IEM-1210, Jeol; Tokyo, Japan).

MOAT

Preparation of mouse oocytes Mature B6D2F1 female mice, 8–12 weeks of age, were superovulated by IP injections of 5 IU pregnant mare serum gonadotropin (PMSG) followed by the administration of 5 IU hCG 48 hours later. The mouse oocytes were collected from the oviducts of the females 14–16 hours after the hCG injection. The oocytes were freed from cumulus cells by pipetting in a Hepes-human follicular fluid medium (Hepes-HFF99; Fuso Pharmaceutical Industries, Osaka, Japan) supplemented with 10% synthetic serum substance (SSS; Irvine Scientific, Santa Ana, CA) and 60 IU/mL bovine testicular hyaluronidase (Sigma Chemical Co., St. Louis) at 37°C. These oocytes were rinsed and kept in an HFF

medium (HFF99; Fuso Pharmaceutical Industries) at 37°C in an atmosphere of 5% CO_2 until the sperm were injected.

Procedures of ICSI and mouse oocyte activation The round-headed sperm of this patient were injected into the mouse oocytes by a piezo-driven unit using the methods reported elsewhere (13–15). The oocyte membranes were broken by applying one or two faint piezo pulses, and the sperm were injected into each ooplasm. It took approximately 20 minutes to inject a group of about 15 oocytes. The injected oocytes were kept for 20–30 minutes at room temperature. During this interval, the oocytes that had been classified into the activation treatment group were activated in a Ca-free Toyoda, Yokoyama, Hoshi (TYH) medium containing 10 mM $SrCl_2$ for 60 minutes at 37°C in an atmosphere of 5% CO_2. These oocytes were transferred one by one into a single 10-μL drop of HFF99 medium with 10% SSS under mineral oil in a plastic dish, and the dish was incubated at 37°C in an atmosphere of 5% CO_2. Approximately 7–11 hours after injections and the activation treatment, the oocytes were observed under an inverted microscope and were rotated to determine whether or not the second polar body and two pronuclei were present.

For the statistical analysis, the obtained data were analyzed by the χ^2-test.

Ovarian Stimulation, Oocyte Collection, and Oocyte Activation in Patient

Ovarian stimulation was conducted using a combination of GnRH agonist (Nasanyl, Yamanouchi, Japan) and hMG (Pergogreen; Serono, Geneva, Swizerland). An injection of 5000 units of hCG (Profasi, Serono) was administered when the dominant follicle reached a mean diameter of 20 mm. Vaginal ultrasound-guided follicle puncture was conducted 36 hours after the hCG injection. The retrieved oocytes were cultured for several hours in Quinn's Advantage Cleavage medium (Sage, Pasadena, CA) at 37°C in an atmosphere of 6% CO_2, 5% O_2, 89% N_2, under humidified conditions, and all oocytes were denuded enzymatically with 70 IU/mL SynVitro Cumulase (MediCult, Copenhagen, Denmark) for 30–60 seconds, followed by mechanical denudation. The motile round-headed sperm were injected into the oocytes in metaphase II, and these oocytes were activated by calcium ionophore A23187 (Sigma;10 μM/mL) for 5 minutes after ICSI. Subsequently, the oocytes were rinsed several times in culture medium and incubated overnight to recognize 2 pronuclei at 37°C in an atmosphere of 6% CO_2, 5% O_2, and 89% N_2 under humidified conditions. For blastocyst cultivation, we transferred the embryos to a sequential medium Quinn Advantage (Sage) or Multi-Blasto Medium (Irvine, CA) on day 3.

Vitrifying and Warming of Blastocysts

All blastocysts were cryopreserved using the vitrification method as described in Kyono et al. (16) to prevent severe ovarian hyperstimulation syndrome (OHSS). The blastocysts were equilibrated for 8–10 minutes in 7.5% ethylene glycol (EG) and 7.5% dimenthyl sulfoxide (DMSO) and then into cryoprotectant 15% EG, 15% DMSO, and 0.5 M sucrose (Kitazato Supply Ltd., Japan) for 1 minute. After that, they were immediately put on a Cryotop and inserted into liquid nitrogen. Warming was performed at room temperature by the rapid thawing method following the market procedure (Kitazato Supply Ltd.). Cryoprotectant was removed by stepwise reduction of the EG and DMSO concentration containing 1.0, 0.5, and 0 M sucrose.

After a single vitrified-warmed blastocyst (grade 5BA) was transferred, a clinical pregnancy was determined by the presence of a gestational sac (GS) and a fetal heartbeat via a transvaginal ultrasound.

RESULTS

The couple did not achieve a pregnancy in spite of repeatedly attempted IUI. We diagnosed the husband as having globozoospermia, which is defined as round-headed sperm lacking an acrosome by the Kruger test and transmission electron microscope (Fig. 1). MOAT was tried but still resulted in no fertilization under piezo-ICSI without activation. As the fertilization rate after $SrCl_2$ activation was increased to 68.4%, it was strongly recommended to pursue the necessary artificial activation to increase the fertilization rate (Table 1).

Round-headed sperm were injected into 17 oocytes during metaphase II. Among the injected oocytes, 15 oocytes were activated (15/17, fertilization rate 88.2%). By day 5, 10 embryos had developed, and another blastocyst developed on the sixth day. Seven of 11 blastocysts were of good morphology, and four blastocysts did not fit the criteria for fair quality. Two months later, one vitrified blastocyst (grade 5BA) was warmed and transferred to the female patient on the fifth day after hormone treatment with P 50 mg (Fuji Pharmaceutical Co., Ltd., Tokyo, Japan). The luteal phase was supported by daily injections of P. After 10 days, pregnancy was established by positive ß-hCG in the serum, and the fetal heartbeat was later confirmed by ultrasound. The couple did not desire amniocentesis so we did not perform it. Fortunately, the female patient remained in good condition throughout the full-term pregnancy. Finally, a healthy boy weighing 3180 g was delivered at 40 weeks of gestation by cesarean section.

DISCUSSION

ICSI is a useful technique for men who are infertile because of round-headed sperm. ICSI has led to fertilization, embryo development, pregnancy, and delivery of infants (1–9). However, several investigators have reported low to absent fertilization (2, 4, 5, 17, 18). Rybouchkin et al. (11) discovered that fertilization was improved when a calcium ionophore was added. They suggested that a sperm-associated oocyte-activating factor that normally causes the Ca^{2+} flux required for fertilization might be absent or down-regulated in globozoospermic sperm, a suggestion that was subsequently confirmed by several studies (11, 19, 20). Subsequently, Rybouchkin et al. in 1997 (18), Kim et al. in 2001 (21),

TABLE 1

Results of injected round-headed sperm to mouse oocytes and activation.

	Activation (+)	Activation (−)
No. of oocytes with ICSI	22	20
No. of surviving oocytes	21	19
Normal morphology	19	19
Abnormal morphology	0	0
2PN 2PB (+)	13 (68.4)	0
2PN 2PB (−)	1 (5.3)	0
1PN 2PB (+)	3 (15.8)	0
3PN 2PB (−)	2 (10.5)	0
0PN 2PB (+)	0	0
0PN 2PB (−)	0	19 (100)
Total activated oocytes	19 (100)	0 (0)

Note: Data in parentheses are percents. Activation (+): The activation treatment group was activated in a Ca-free TYH medium containing 10 mM $SrCl_2$ for 60 minutes at 37°C in an atmosphere of 5% CO_2. The details are mentioned in Materials and Methods. 2PN = two pronuclei formation; 2PB = first and second polar body.

Kyono. Birth from a globozoospermic patient. Fertil Steril 2009.

Heindryckx et al. in 2005 (15), and Tajera et al. in 2008 (22) reported successful pregnancies and deliveries using ICSI with calcium ionphore oocyte activation. On the other hand, Tesarik et al. in 2002 (14) reported that the possibility of using a simple modification of the standard ICSI micromanipulation technique, instead of ionophores, alleviates concerns about the possible harmful effects to human embryos of these insufficiently tested drugs. Vigorous aspiration of oocyte cytoplasm and repeated in-and-out movements of the microinjection needle within the human oocyte during the ICSI produce a considerable influx of calcium ions from the surrounding culture medium into the oocyte. It is also possible that mechanical disruption of endoplasmic reticulum during the movements of the microinjection needle in the oocyte cytoplasm and repeated aspiration releases the calcium stored in this organelle. The modified ICSI technique increases the intracellular concentrations of the free calcium ion in the injected oocyte compared with the standard ICSI technique.

Electrical stimulation, ethanol, $SrCl_2$, Ca ionophore, and vigorous ICSI have been reported as AOA. Ca ionophore, ethanol 8%, and $SrCl_2$ (from our data) displayed the efficacy of AOA for globozoospermia in heterologous ICSI models. Ca ionophore and vigorous ICSI were reported to have the effectiveness of AOA for globozoospermia in human ICSI clinically, but electrical stimulation, ethanol, and $SrCl_2$ are not yet reported to be effective. More studies are needed to examine which method is truly the best for AOA in globozoospermia.

This couple had tried IUI three times; however, they did not achieve pregnancy. First, we diagnosed the husband as having globozoospermia. Second, we compared the results with and without oocyte activation using $SrCl_2$ on mouse oocytes with round-headed sperm injection. From the outcomes of MOAT, we concluded that round-headed sperm might lack the ability of oocyte activation. We reported the efficacy and the safety of $SrCl_2$ in the patients with low fertilization by ICSI (23). However, the $SrCl_2$ activator is not yet approved for use with human oocytes in the case of globozoospermia. Third, in this case, we tried calcium ionophore A23187 treatment, which was also reported by several investigators (18, 19, 22, 23) to activate human oocytes injected with round-headed sperm. The fertilization rate in our case is 82.2% (15 of 17), which may be attributed to the AOA with calcium ionophore A23187 treatment. We believe that oocyte activation after ICSI using round-headed sperm is vital.

Edirisinghe et al. (24) studied the cytogenetics of unfertilized oocytes after ICSI. Failure of activation and the consequent failure of the oocyte to complete meiosis II were likely to have contributed to the high rate of premature chromatin condensation seen in their cases. These data suggest that round-headed sperm lack the capacity to penetrate oocytes and may also be deficient in their oocyte-activating ability.

Generally, round-headed sperm were observed to have a comparatively higher chance of abnormal aneuploidy chromosome (25–27), and chromatin structure and centrosomal function had activated abnormally in globozoospermia (28–30).

Although karyotypes of round-headed sperm have not been discussed in many nuclear studies in great detail, several articles have reported on aneuploidy, centrosomal dysfunction, and chromatid structure abnormalities. More studies regarding the karyotypes of rounded-headed sperm are necessary in the future. Round-headed sperm are deficient in oocyte-activation capacity, and this deficiency is independent of the variation in morphology of the sperm heads. The most probable reason for this deficiency is the absence or down-regulation of the sperm oocyte-activating factor in these sperm. Further investigation of globozoospermia would give valuable information on the general mechanism of spermatogenesis; different aspects of sperm-egg interaction; and physiology, etiology, and chromosome aneuploidy of globozoospermia.

In summary, we report a successful pregnancy and delivery from a transfer of a single vitrified-warmed blastocyst after performing ICSI with round-headed sperm and AOA in a globozoospermic patient.

REFERENCES

1. Lundin K, Sjogren A, Nilsson L, Hamberger L. Fertilization and pregnancy after intracytoplasmic microinjection of acrosomeless spermatozoa. Fertil Steril 1994;62:1266–7.
2. Liu J, Nagy Z, Joris H, Tournaye H, Devroey P, Van Steirteghem A. Successful fertilization and establishment of pregnancies after intracytoplasmic sperm injection in patients with globozoospermia. Hum Reprod 1995;10:626–9.
3. Trokoudes KM, Danos N, Kalogirou L, Vlachou R, Lysiotis T, Georghiades N, et al. Pregnancy with spermatozoa from a globozoospermic man after intracytoplasmic sperm injection treatment. Hum Reprod 1995;10:880–2.
4. Kilani ZM, Shaban MA, Ghunaim SD, Keilani SS, Dakkak AI. Triplet pregnancy and delivery after intracytoplasmic injection of round-headed spermatozoa. Hum Reprod 1998;13:2177–9.
5. Stone S, O'Mahony F, Khalaf Y, Taylor A, Braude P. A normal live birth after intracytoplasmic sperm injection for globozoospermia without assisted oocyte activation. Hum Reprod 2000;15:139–41.
6. Coetzee K, Windt ML, Menkveld R, Kruger TF, Kitshoff M. An intracytoplasmic sperm injection pregnancy with a globozoospermic male. J Assist Reprod Genet 2001;18:311–3.
7. Nardo LG, Sinatra F, Bartoloni G, Zafarana S, Nardo F. Ultrastructural features and ICSI treatment of severe teratozoospermia: report of two human cases of globozoospermia. Eur J Obstet Gynecol Reprod Biol 2002;104:40–2.
8. Zeyneloglu HB, Baltaci V, Duran HE, Erdemli E, Batioglu S. Achievement of pregnancy in globozoospermia with Y chromosome microdeletion after ICSI. Hum Reprod 2002;17:1833–6.
9. Kilani Z, Ismail R, Ghunaim S, Mohamed H, Hughes D, Brewise I, et al. Evaluation and treatment of familial globozoospermia in five brothers. Fertil Steril 2004;82:1436–9.
10. Dam AH, Frenstra I, Westphal JR, Ramos L, Van Golde RJ, Kremer JA. Globozoospermia revisited. Hum Reprod Update 2007;13:63–75.
11. Rybouchkin AV, Dozortsev D, Pelinck MJ, De Sutter P, Dhont M. Analysis of the oocyte activating capacity and chromosomal complement of round-headed human spermatozoa by their injection into mouse oocytes. Hum Reprod 1996;11:2170–5.
12. Abe H, Otoi T, Tachikawa S, Yamashita S, Satoh T, Hopshi H. Fine structure of bovine morulae and blastocysts in vivo and in vitro. Anat Embryol 1999;199:519–27.
13. Araki Y, Yoshizawa M, Abe H, Murase Y, Araki Y. Use of mouse oocytes to evaluate the ability of human sperm to activate oocytes after failure of activation by intracytoplasmic sperm injection. Zygote 2004;12:111–6.
14. Tesarik J, Rienzi L, Ubaldi F, Mendoza C, Greco E. Use of a modified intracytoplasmic sperm injection technique to overcome sperm-borne and oocyte-borne oocyte activation failures. Fertil Steril 2002;78: 619–24.
15. Heindryckx B, Van del Elst J, De Sutter P, Dhont M. Treatment option for sperm- or oocyte-related fertilization failure: assisted oocyte activation following diagnostic heterologous ICSI. Hum Reprod 2005;20: 2237–41.
16. Kyono K, Nakajo Y, Kumagai S, Nishinaka C. Vitrifying and warming of oocytes using cryotop. In: Tucker MJ, Liebermann J, eds. Vitrification in Assisted Reproduction. A User's Manual and Trouble-Shooting Guide: Informa UK Ltd., 2007:153–61.
17. Battaglia DE, Koehler JK, Klein NA, Tucker MJ. Failure of oocyte activation after intracytoplasmic sperm injection using round-headed sperm. Fertil Steril 1997;68:118–22.
18. Rybouchkin AV, Van der Straeten F, Quatacker J, De Sutter P, Dhont M. Fertilization and pregnancy after assisted oocyte activation and intracytoplasmic sperm injection in a case of round-headed sperm associated with deficient oocyte activation capacity. Fertil Steril 1997;68:1144–7.
19. Gomez E, Perez-Cano I, Amorocho B, Landeras J, Ballesteros A, Pellicer A. Effect of injected spermatozoa morphology on the outcome of intracytoplasmic sperm injection in humans. Fertil Steril 2000;74: 842–3.
20. Schmiady H, Schulze W, Scheiber I, Pfuller B. High rate of premature chromosome condensation in human oocytes following microinjection with round-headed sperm: case report. Hum Reprod 2005;20: 1319–23.
21. Kim ST, Cha YB, Park JM, Gye MC. Successful pregnancy and delivery from frozen-thawed embryos after intracytoplasmic sperm injection using round-headed spermatozoa and assisted oocyte activation in a globozoospermic patient with mosaic Down syndrome. Fertil Steril 2001;75: 445–7.
22. Tajera A, Molla M, Muriel L, Remohi J, Pellicer A, De Pablo JL. Successful pregnancy and childbirth after intracytoplasmic sperm injection with calcium ionophore oocyte activation in a globozoospermic patient. Fertil Steril 2008;90:1202.e1–e5.
23. Kyono K, Kumagai S, Nishinak C, Nakajo Y, Uto H, Toya M, et al. Birth and follow-up of babies born following ICSI using SrCl2 oocyte activation. RBM Online 2008;17:53–8.
24. Edirisinghe WR, Murch AR, Junk SM, Yovich JL. Cytogenetic analysis of unfertilized oocytes following intracytoplasmic sperm injection using spermatozoa from a globozoospermic man. Hum Reprod 1998;13: 3094–8.
25. Martin RH, Greene C, Rademaker AW. Sperm chromosome aneuploidy analysis in a man with globozoospermia. Fertil Steril 2003;79(Suppl 3): 1662–4.
26. Morel F, Douet-Guilbert N, Moerman A, Duban B, Marchetti C, Delobel B, et al. Chromosome aneuploidy in the spermatozoa of two men with globozoospermia. Mol Hum Reprod 2004;10:835–8.
27. Ditzel N, El-Danasouri I, Just W, Sterzik K. Higher aneuploidy rates of chromosomes 13, 16, and 21 in a patient with globozoospermia. Fertil Steril 2005;84:217–8.
28. Vicari E, Perdichizzi A, De Palma A, Burrello N, D'Agata R, Calogero AE. Globozoospermia is associated with chromatin structure abnormalities: case report. Hum Report 2002;17:2128–33.
29. Larson KL, Brannian JD, Singh NP, Burbach JA, Jost LK, Hansen KP, et al. Chromatin structure in globozoospermia: a case report. J Androl 2001;22:424–31.
30. Nakamura S, Terada Y, Horiuchi T, Emuta C, Murakami T, Yaegashi N, et al. Analysis of the human sperm centrosomal function and the oocyte activation ability in a case of globozoospermia, by ICSI into bovine oocytes. Hum Reprod 2002;17:2930–4.

Analytical Biochemistry 385 (2009) 138–142

Contents lists available at ScienceDirect

Analytical Biochemistry

journal homepage: www.elsevier.com/locate/yabio

A microfluidic dual capillary probe to collect messenger RNA from adherent cells and spheroids

Hitoshi Shiku [a,*], Takeshi Yamakawa [a], Yuji Nashimoto [a], Yasufumi Takahashi [a], Yu-suke Torisawa [a], Tomoyuki Yasukawa [a], Takahiro Ito-Sasaki [b], Masaki Yokoo [c], Hiroyuki Abe [b], Hideki Kambara [d,e], Tomokazu Matsue [a,*]

[a] Graduate School of Environmental Studies, Tohoku University, Aobe 6-6-11-604, Sendai 980-8579, Japan
[b] Graduate School of Science and Engineering, Yamagata University, Yonezawa 992-8510, Japan
[c] Innovation of New Biomedical Engineering Center, Tohoku University, Sendai 980-8574, Japan
[d] Central Research Laboratory, Hitachi, Kokubunji, Tokyo 185-8601, Japan
[e] Tokyo University of Agriculture and Technology, Koganei, Tokyo 184-8588, Japan

ARTICLE INFO

Article history:
Received 3 September 2008
Available online 5 November 2008

Keywords:
RT-PCR
Real-time PCR
Microfluidics
Single cell analysis

ABSTRACT

Collection of bioanalytes from single cells is still a challenging technology despite the recent progress in many integrated microfluidic devices. A microfluidic dual capillary probe was prepared from a theta (θ)-shaped glass capillary to analyze messenger RNA (mRNA) from adherent cells and spheroids. The cell lysis buffer solution was introduced from the injection aperture, and the cell-lysed solution from the aspiration aperture was collected for further mRNA analysis based on reverse transcription real-time PCR. The cell lysis buffer can be introduced at any targeted cells and never spilled out of the targeted area by using the microfluidic dual capillary probe because laminar flow was locally formed near the probe under the optimized injection/aspiration flow rates. This method realizes the sensitivity of mRNA at the single cell level and the identification of the cell types on the basis of the relative gene expression profiles.

Hydrodynamics is an important aspect for controlling the mass transfer of reagents and has been combined with various analytical tools such as electrochemical [1–5], electrophoretic [6–8], and chromatographic [9] instruments. Recently, the concept of a micro-total analysis system (μTAS)[1] has been receiving attention in analytical chemistry to realize integration of parallel and sequential operations on a solid substrate [10–13]. Microfluidic devices have rendered possible the guiding of chemicals based on laminar flow [14–18]. This technology has been applied for local patterning of proteins [14], targeted delivery of cells, and removal of attached cells [15,16]. However, for most chip designs, microfluidics has currently been constructed in "closed" channels based on the lab-on-a-chip concept. Delamarche and coworkers invented the remarkably innovative microfluidic probe (MFP) that can be applied in "open" space and, therefore, can form a focused laminar flow at any site for protein patterning, cell lysing, and injecting fluorescent dyes into target cells [19,20]. The original MFP possessed a mesa structure prepared with a silicon chip and two apertures for injection and aspiration.

In the current study, we first applied the MFP technology for collection of messenger RNA (mRNA) from single adherent cells. The probe has been constructed with a dual pipette and comprised a theta (θ)-shaped glass capillary. Pulled glass capillaries [21–24] and dual pipette probes [25–30] have been used in various analytical tools with micromanipulators, including physiology, capillary electrophoresis, and electrochemistry, as well as for various scanning probe microscopies (SPMs). An exclusive characteristic of MFP allows the aspirated sample solution to be used for further analysis, similar to that in perfusion or microdialysis. We collected mRNA from monolayer-cultured cells, namely the human breast cancer cell line MCF-7 and the malignant human mammary epithelial cell line HMT-3522 T4-2 (T4-2) [31,32], using the probe for injecting a lysis buffer and aspirating the lysed cytosol. The collection efficiency of the mRNA was evaluated quantitatively using real-time PCR. This technique has a significant impact in the research field of single cell analysis because the collection process is the bottleneck to automatically perform sequential chemical processing on an integrated μTAS device. We focused on the expression levels of β1-integrin, a major protein to regulate cell–cell and cell–ECM (extracellular matrix) interactions, because the microfluidic dual capillary probe is principally applicable to collect

* Corresponding authors. Fax: +81 22 217 7209.
E-mail addresses: shiku@bioinfo.che.tohoku.ac.jp (H. Shiku), matsue@bioinfo.che.tohoku.ac.jp (T. Matsue).

[1] *Abbreviations used:* μTAS, micro-total analysis system; MFP, microfluidic probe; mRNA, messenger RNA; SPM, scanning probe microscopy; T4-2, HMT-3522 T4-2; ECM, extracellular matrix; DMEM, Dulbecco's modified Eagle's medium; PCR, polymerase chain reaction; RNase, ribonuclease; RT, reverse transcription; cDNA, complementary DNA; GAPDH, glyceraldehyde-3-phosphate dehydrogenase.

0003-2697/$ - see front matter © 2008 Elsevier Inc. All rights reserved.
doi:10.1016/j.ab.2008.10.039

adherent cells and spheroids at any position. It is already known that β1-integrin expression for MCF-7 is significantly smaller than that for T4-2. Also, it is known that β1-integrin expression for spheroid culture is larger than that for monolayer culture. Therefore, as a model system, MCF-7 and T4-2 cell lines cultured in monolayer and spheroid cultures were selected for the mRNA analysis samples.

Materials and methods

Microfluidic dual capillary probe

A theta-shaped borosilica glass tube (1.5 mm o.d., 1.02 mm i.d., TST150-6, World Precision Instruments) was cut to a length of 50 mm and pulled with a capillary puller (PN-3, Narishige). The top of the dual pipette capillary was then planed with a diamond grinder (EG-6, Narishige) to fabricate a disk-shaped tip with an outer diameter of 40 to 100 μm (Fig. 1). It was difficult to prepare the probes with precisely the same orifice size.

The bottom of the dual pipette probe was connected to the two silica capillary tubes (25 cm in length, 0.375 mm o.d., 0.075 mm i.d., 31942, GL Science) by using epoxy glue. The two microsyringes, syringe 1 (used for injection) and syringe 2 (used for aspiration), were connected tightly with the silica capillary tube with a special adaptor set (Upchurch Scientific).

Cell culture

Methods for monolayer culture [33] and three-dimensional culture on reconstructed basement membrane (on-top culture) [34] have been described elsewhere [35]. The human breast cancer cell line (MCF-7) was donated by the Cell Resource Center for Biomedical Research (Tohoku University). The malignant human mammary epithelial cell line (T4-2) [32] was obtained from the American Type Culture Collection. RPMI 1640 medium (Gibco) containing 10% fetal bovine serum (FBS, Gibco), 50 μg ml^{-1} penicillin (Gibco), and 50 μg ml^{-1} streptomycin (Gibco) was used for MCF-7 culture. Dulbecco's modified Eagle's medium (DMEM)/F12 medium (Gibco) containing 250 ng ml^{-1} insulin (Boehringer Mannheim), 10 μg ml^{-1} transferrin (Sigma), 2.6 ng ml^{-1} sodium selenite (Collaborative Research), 0.1 nM estradiol (Sigma), 1.4 μM hydrocortisone (Collaborative Research), and 5 μg ml^{-1} prolactin (Sigma) was used for culturing T4-2. For monolayer culture, The bottom of a 35-mm polystyrene culture dish (BD Biosciences) was coated with type 1 collagen solution (Research Institute for the Functional Peptides) by incubation for more than 30 min. Cells were seeded onto the collagen-coated dish as a single cell suspension. For on-top culture, the bottom of a 35-mm polystyrene culture dish was initially coated with 30 μl of Matrigel (BD Biosciences). The Matrigel coated on the culture dish was solidified at 37 °C for 10 min. Single cells were seeded on the layer of the Matrigel with 50 μl of 1 to 5 × 10^4 cells/ml cell suspension in medium solution containing 2% Matrigel. Single cells were adherent onto the Matrigel layer after 30 to 60 min incubation at 37 °C. The culture dish was further filled with the medium containing 2% Matrigel. Cells proliferate and form spheroids after 3 days.

Cell lysis and mRNA collection with the microfluidic dual capillary probe

The probe was silanized with a 50-μl drop of 4,4,5,5,6,6,6-nonafluorohexyltrichlorosilane (LS-912, Shin-etsu Chemical) evaporated in a closed 200-ml beaker under a nitrogen atmosphere at room temperature for 2 h. The probe and the two syringes were washed with 99.6% ethanol. The probe was set on an XYZ stage, and the two syringes were controlled with syringe pumps (KDS200&KDS230, Muromachi). The distance between the probe and the sample was defined by gently touching the bottom of the culture dish, and the probe was retracted 20 μm apart from the bottom using a motor-driven XYZ stage and a stage controller (D73MS, Suruga Seiki). Then the probe was located at the center of the microscope view.

Cell extraction using microfluidic dual capillary probe

Fig. 1 shows a scheme of the experimental setup. The lysis buffer RLT (50 μl, RNeasy Micro Kit, Qiagen) was roared into the injection syringe (syringe 1) and the aspiration syringe (syr-

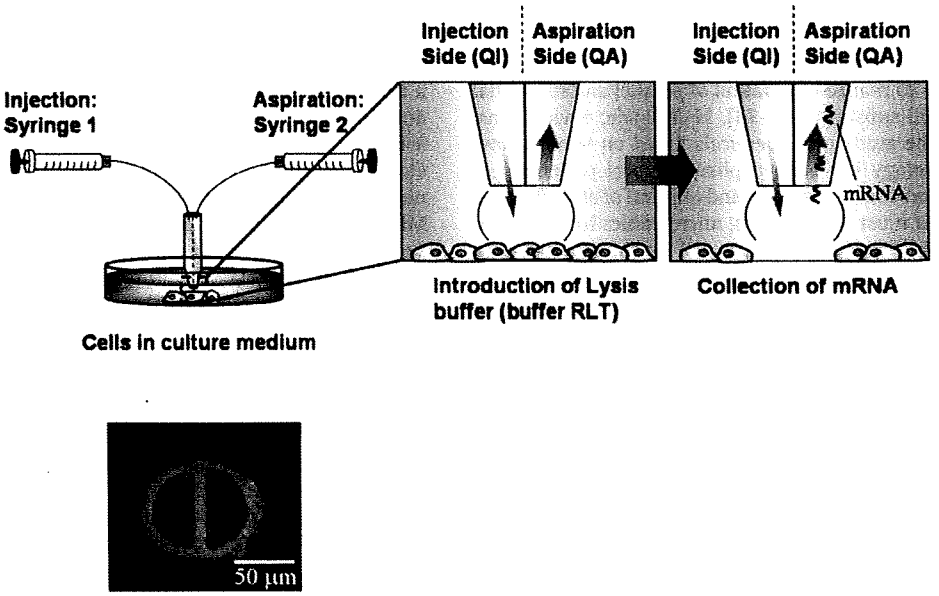

Fig. 1. Scheme of the experimental setup. QI (injection flow rate) and QA (aspiration flow rate) were set at 40 and 360 nl/min, respectively. The flow rate ratio (QA/QI) was set at 9. A bottom view of the theta-shaped microfluidic dual capillary probe is also shown.

inge 2). mRNA was collected from MCF-7 monolayer cells by using the microfluidic dual capillary probe. The injection (QI) and aspiration (QA) flow rates were set at 40 and 360 nl/min, respectively. The flow rate ratio (QA/QI) was 9 [19]. After the observation of cellular lysis and removal from the culture dish, the probe was transferred into another dish filled with 2 ml of buffer RLT and further aspirated at 5 μl/min for 10 min. Initially, syringe 2 was loaded with 50 μl of buffer RLT; thus, the final volume of the collected cell-lysed solution with syringe 2 resulted in approximately 150 μl. The collected cell lysate solution was poured out into a 0.2-ml polymerase chain reaction (PCR) tube. Then 5 μl of the 4 ng/μl carrier RNA (Qiagen) was added into the PCR tube for preventing the degradation of the targeted RNA originating from contaminated ribonuclease (RNase). The carrier RNA also guards the adsorption of the targeted RNA onto the PCR tube.

The solution in the PCR tube was then purified using an RNeasy Micro Kit (Qiagen). Reverse transcription (RT) reaction and real-time PCR were performed using a QuantiTect Reverse Transcription Kit (Qiagen) and a LightCycler FastStart DNA Master Kit (Roche), respectively. The real-time PCR (LightCycler 1.5, Roche) was performed for at least two genes using 2 μl of the sample complementary DNA (cDNA) taken from 20 μl of the synthesized source cDNA solution. The running conditions have been described elsewhere [35]. Primers for glyceraldehyde-3-phosphate dehydrogenase (GAPDH, GenBank Accession No. M33197) and β1-integrin (GenBank Accession No. NM_133376) were designed and synthesized by Nihon Gene Research Laboratories. The actual sequences, apricon sizes, and annealing temperatures of the primers were listed as follows: GAPDH, forward 5′-TGA ACG GGA AGC TCA CTG G-3′, reverse 5′-TCC ACC ACC CTG TTG CTG TA-3′, 307 bp, 62 °C; β1-integrin, forward 5′-GTC CAA CCT GAT CCT GTG TC-3′, reverse 5′-GCA ACC ACA CCA GCT ACA AT-3′, 167 bp, 66 °C. The precise GAPDH copy number was determined using a standard plasmid DNA-containing GAPDH synthesized by Nihon Gene Research Laboratories. We also performed bulk measurement using 10^5 to 10^6 cells as a starting sample. In this case, an RNeasy Mini Kit (Qiagen) was used for RNA purification. For the monolayer cultured cell sample, the medium (RPMI 1640 or DMEM/F12) of the culture dish was changed to the cell lysis buffer RLT (Quiagen), and the lysate was further analyzed to estimate the relative β1-integrin expression level normal to GAPDH for each cell type. The process for spheroid lysis and mRNA extraction was basically the same as that for the monolayer adherent cells.

Results and discussion

Fig. 2A shows the sequential photographs of the sample MCF-7 monolayer cultured on a 35-mm polystyrene dish before and after the cellular collection using the dual capillary probe at a probe–sample distance of 20 μm. Initially, syringe 2 was turned on to aspirate the culture medium from aperture 2 at a flow rate of 360 nl/min (QA). Syringe 1 was immediately used to inject the cell lysis buffer from aperture 1 at a flow rate of 40 nl/min (QI). This protocol ensured that cell lysis buffer solution never spilled out of the targeted area. As seen in Fig. 2A, the target cells were removed within 30 s and the number of lysed cells was found to be 11. The margins of the removed cells are nearly intact, ensuring that the cell lysis buffer attacks only the targeted area during laminar flow when introduced and never leaks out of the targeted area. In the same manner, one cell collection was demonstrated from adherent MCF-7 cells seeded with a lower cellular density (Fig. 2B).

Fig. 3 shows the time course during the real-time PCR operation and the melting curve analysis performed after the real-time PCR for β1-integrin mRNA sample collected from MCF-7 monolayer. These results were obtained from 11 cells and 1 cell using the microfluidic dual capillary probe corresponding to the photographs shown in Fig. 2A and B, respectively. The peak in the melting curve was well correlated with the signal obtained for the bulk of cellular samples with 10^5 to 10^6 cells.

The copy number of the GAPDH, which was collected from the MCF-7 monolayer (including 1–17 cells, $n = 6$) by using the probe, was 76.7 copies/cell. This value corresponded to the apparent collection efficiency 7.6% because the copy number estimated using bulk measurement ($\sim 10^6$ cells) was 1014 copies/cell. This low efficiency is due to the instability of the mRNA; the expected collection efficiency with QA/QI = 9 was approximately 100%, as shown in the literature [19]. In our case, the collection efficiency of approximately 100% was achieved for a QA/QI value larger than 8 when a solution containing 10^5 particles/ml of 6-μm-diameter microspheres (Polysciences) was introduced through the microfluidic dual capillary probe. The concentration of the product (mRNA) should be high; thus, the QA/QI value cannot be set at an undesirably larger value for our objective, that is, mRNA collection. The smaller the gap distance becomes, the larger the expected collection efficiency increases. The orifice size did not seem to affect the collection efficiency of the mRNA. The microfluidic dual capillary probe with less than 10 μm diameter can be fabricated, and we observed that a part of the MCF-7 spheroid was lysed with the smaller probe. However, in the current stage, we have not succeeded in RNA analysis with the smaller probe.

The retention time of the cell-lysed solution including mRNA and buffer RLT within the aspiration side compartment of the probe is 38 min, which is estimated from the volume of the aspiration side compartment (13.7 μl, a half-volume of the dual capillary probe) and the QA value (360 nl/min). This time scale is significantly large compared with the actual time period taken for the process of cell lysis (30 s), implying that the collected mRNA remains in the probe compartment but does not reach syringe 2. During the cell lysis, buffer RLT is diluted to approximately 10% of the original concentration, and this may be the main reason for the mRNA degradation given the roles that buffer RLT plays in RNase deactivation and RNA stabilization. After the cell lysis process, the probe was transferred into a buffer RLT pool and further aspirated with 50 μl (see Materials and Methods). In this step, the cell-lysed sample surely reaches syringe 2, where the concentration of buffer RLT recovers to the original one because the volume of the cell-lysed sample (180 nl) is negligibly small compared with the total volume of buffer RLT (150 μl).

Although the mRNA collection efficiency was low in the current stage, comparison of the gene expression at individual cell level was possible. Expression of β1-integrin for MCF-7 and T4-2 collected using the microfluidic dual capillary probe was surveyed normal to that of GAPDH for each. Fig. 4 reveals the relative β1-integrin expression for a small number of adherent cells (1 to 17 MCF-7 cells [$n = 6$] and 1 T4-2 cell [$n = 3$] cultured with monolayer). The β1-integrin expression for the T4-2 cells was approximately 10-fold greater than that for the MCF-7 cells. The results obtained using the current method with the microfluidic dual capillary probe are similar to those obtained using a conventional method based on the collection of bulk cells ($\sim 10^6$ cells), indicating that the current method provided quantitative information regarding the expression levels of the target gene in the two cell lines. T4-2 expresses β1-integrin at substantially higher level than does MCF-7 [31]. Although our theta-shaped probe was very easy to fabricate, the performance was comparable to that achieved by a sophisticated MFP [19].

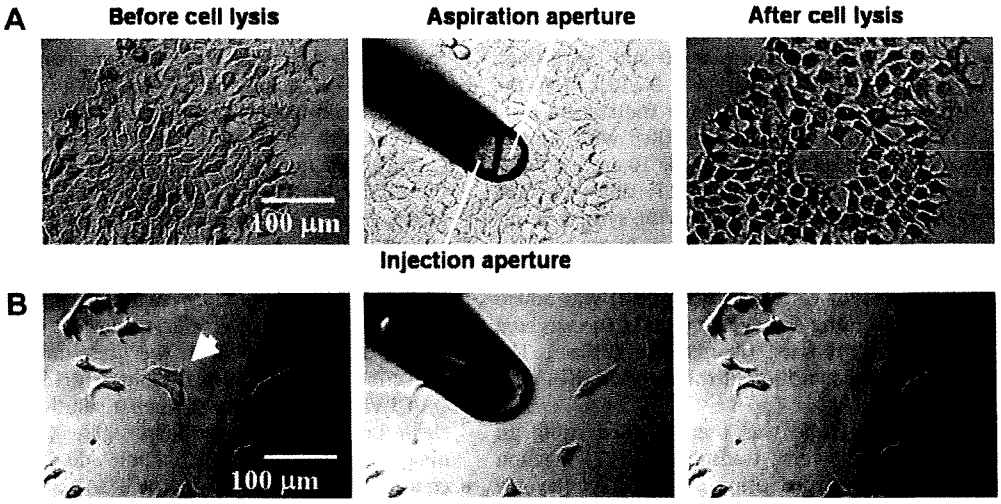

Fig. 2. (A) Sequential photos of MCF-7 monolayer before and after the RNA collection using the microfluidic dual capillary probe. The injection (QI) and aspiration (QA) flow rates were set at 40 and 360 nl/min, respectively. The distance between the probe and the bottom of the culture dish was set at 20 μm. It takes 10 to 30 s for the cell lysis to be completed, and the total volume of the cell-lysed solution was approximately 150 μl. From this picture, 11 cells were collected to further mRNA analysis. (B) In the same manner, the single cell collection was available from adherent MCF-7 cells seeded with a lower cellular density.

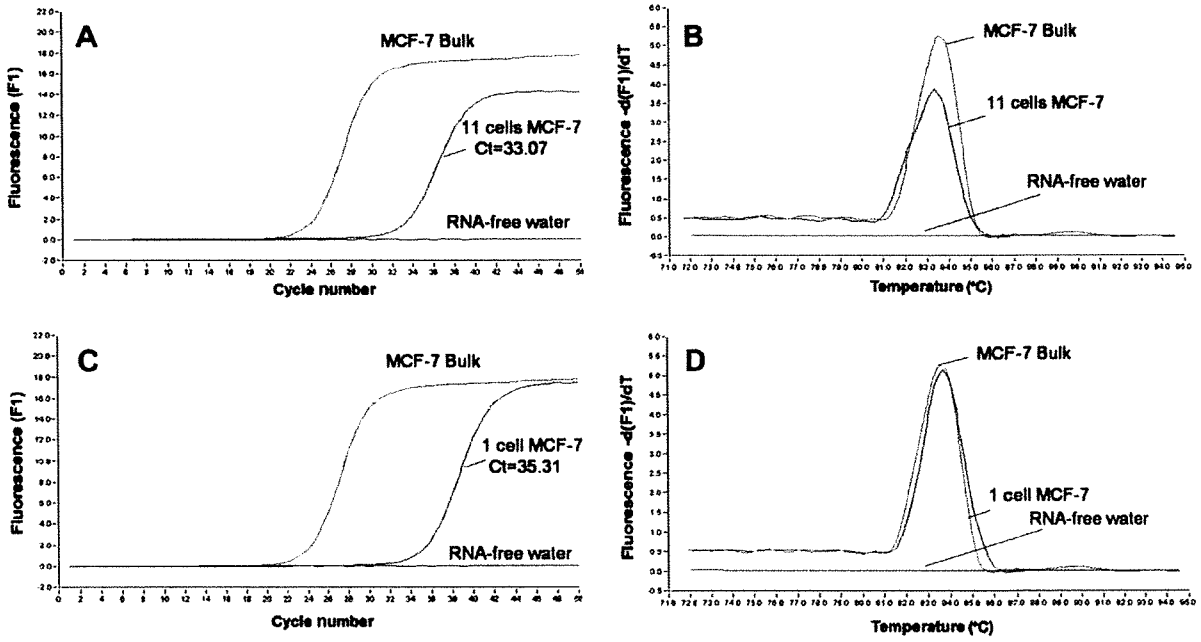

Fig. 3. Time course of the fluorescence intensity during the real-time PCR operation (A and C) and melting curve analysis performed after real-time PCR (B and D) for the β1-integrin mRNA sample collected from MCF-7 monolayer (11 cells [A and B] and 1 cell [C and D] shown in Fig. 2) using the microfluidic dual capillary probe.

Moreover, our method enabled collection of mRNA from a single spheroid, namely, an aggregated cellular mass in a three-dimensional cultures system. MCF-7 and T4-2 cells were cultured onto a Matrigel sheet to form a spheroid 3 days after the single cell seeding. Initially, we tried to pick one cell or several cells from a spheroid using the microfluidic dual capillary probe, but it was difficult to lyse a part of the single spheroid with a diameter of 100 μm. Fig. 5 shows the relative β1-integrin expression from single spheroids (MCF-7 [$n = 4$] and T4-2 [$n = 2$]). The β1-integrin expression for the spheroid was identical to, or a little bit larger than, that cultured with monolayer for both cell types. The results obtained for bulk measurement (~8000 spheroids) were in good agreement with those obtained for individual spheroids collected using the theta-shaped probe. Again, the results of the relative gene expression profiles clearly identified the differences between the two cell types.

Conclusions

In conclusion, MFP technology has been applied, for the first time, for the mRNA collection and analysis of single adherent cells and single spheroids. The collection efficiency was estimated as 7.6% using the GAPDH mRNA from single MCF-7 cells. Using the current method, a quantitative discussion is possible to distinguish

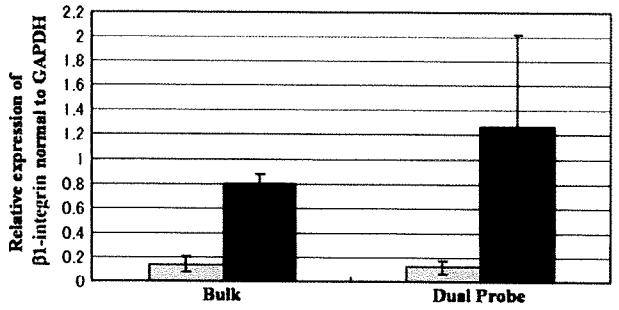

Fig. 4. Relative expression levels of β1-integrin normal to GAPDH for MCF-7 cells (gray bars) and T4-2 cells (filled bars) cultured with monolayer. mRNA collected from bulk (~10^6 cells) (left) and the microfluidic dual capillary probe (right).

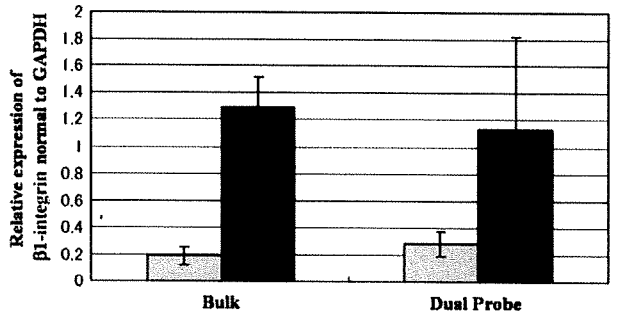

Fig. 5. Relative expression levels of β1-integrin normal to GAPDH in spheroids for MCF-7 cells (gray bars) and T4-2 cells (filled bars) three-dimensionally cultured for 3 days onto a Matrigel sheet. mRNA was collected from bulk (~8000 spheroids) (left) and the microfluidic dual capillary probe (1 spheroid) (right).

the difference in the gene expression levels between the two cell lines: MCF-7 and T4-2. The current method is also applicable to mRNA analysis in a three-dimensional culture system.

Acknowledgments

This work was supported partly by a Grant-in-Aid for Scientific Research on Priority Areas (445), "Life Surveyor," from the Ministry of Education, Culture, Sports, Science, and Technology (MEXT) of Japan; by Grants-in-Aid for Scientific Research (18101006 and 19750055) from MEXT; and by a research grant from the Center for Interdisciplinary Research at Tohoku University.

References

[1] P.R. Unwin, Dynamic electrochemistry as a quantitative probe of interfacial physicochemical processes, J. Chem. Faraday Trans. 94 (1998) 3183–3195.
[2] J.V. Macpherson, P.R. Unwin, Hydrodynamic modulation voltammetry with an oscillating microjet electrode, Anal. Chem. 71 (1999) 4642–4648.
[3] O. Niwa, R. Kurita, Z. Liu, T. Horiuchi, K. Torimitsu, Subnanoliter volume wall-jet cells combined with interdigitated microarray electrode and enzyme modified planar microelectrode, Anal. Chem. 72 (2000) 949–955.
[4] A. Aoki, T. Matsue, I. Uchida, Electrochemical response at microarray electrodes in flowing streams and determination of catecholamines, Anal. Chem. 62 (1990) 2206–2210.
[5] T. Matsue, A. Aoki, E. Ando, I. Uchida, Multichannel electrochemical detection system for flow analysis, Anal. Chem. 62 (1990) 407–409.
[6] H. Kambara, S. Takahashi, Multiple-sheathflow capillary array DNA analyzer, Nature 361 (1993) 565–566.
[7] S. Takahashi, K. Murakami, T. Anazawa, H. Kambara, Multiple sheath-flow gel capillary-array electrophoresis for multicolor fluorescent DNA detection, Anal. Chem. 66 (1994) 1021–1026.
[8] C.E. Lunte, P.T. Kissinger, R.E. Shoup, Difference mode detection with thin-layer dual-electrode liquid chromatography/electrochemistry, Anal. Chem. 57 (1985) 1541–1546.
[9] R.T. Kennedy, M.D. Oates, B.R. Cooper, B. Nickerson, J.W. Jorgenson, Microcolumn separations and the analysis of single cells, Science 246 (1989) 57–63.
[10] C.E. Sims, N.L. Allbritton, Analysis of single mammalian cells on-chip, Lab Chip 7 (2007) 423–440.
[11] P.S. Dittrich, K. Tachikawa, A. Manz, Micro total analysis systems: Latest advancements and trends, Anal. Chem. 78 (2006) 3887–3907.
[12] G. Jiang, D.J. Harrison, MRNA isolation in a microfluidic device for eventual integration of cDNA library construction, Analyst 125 (2000) 2176–2179.
[13] G.M. Whitesides, The origins and the future of microfluidics, Nature 442 (2006) 368–373.
[14] E. Delamarche, A. Bernard, H. Schmid, B. Michel, H. Biebuyck, Patterned delivery of immunoglobulins to surfaces using microfluidic networks, Science 276 (1997) 779–781.
[15] S. Takayama, J.C. McDonald, E. Otsuni, M.N. Liang, P.J.A. Kenis, R.F. Ismagilov, G.M. Whitesides, Patterning cells and their environments using multiple laminar fluid flows in capillary networks, Proc. Natl. Acad. Sci. USA 96 (1999) 5545–5548.
[16] Y.C. Tung, Y.S. Torisawa, N. Futai, S. Takayama, Small volume low mechanical stress cytometry using computer-controlled Braille display microfluidics, Lab Chip 7 (2007) 1497–1503.
[17] H. Kaji, M. Nishizawa, T. Matsue, Localized chemical stimulation to micropatterned cells using multiple laminar fluidic flows, Lab Chip 3 (2003) 208–211.
[18] A.M. Taylor, M. Blurton-Jones, S.W. Rhee, D.H. Criccs, C.W. Cotman, N.L. Jeon, A microfluidic culture platform for CNS axonal injury, Regen. Trans. Nat. Methods 2 (2005) 599–605.
[19] D. Juncker, H. Schmid, E. Delamarche, Multipurpose microfluidic probe, Nat. Mater. 4 (2005) 622–628.
[20] E. Delamarche, D. Juncker, H. Schmid, Microfluidics for processing surfaces and miniaturizing biological assays, Adv. Mater. 17 (2005) 2911–2933.
[21] A. Bruckbauer, D. Zhou, L. Ying, Y.E. Korchev, C. Abell, D. Klenerman, Multicomponent submicron features of biomolecules created by voltage controlled deposition from a nanopipet, J. Am. Chem. Soc. 125 (2003) 9834–9839.
[22] J. Olfosson, M. Levin, A. Stromberg, S.G. Weber, F. Rytten, O. Orwar, Scanning electroporation of selected areas of adherent cell cultures, Anal. Chem. 79 (2007) 4410–4418.
[23] Y. Takahashi, Y. Hirano, T. Yasukawa, H. Shiku, H. Yamada, T. Matsue, Topographic, electrochemical, and optical images using standing approach mode scanning electrochemical/optical microscopy, Langmuir 22 (2006) 10299–10306.
[24] A.D. Modestov, S. Srebnik, O. Lev, J. Gun, Scanning capillary microscopy/mass spectrometry for mapping spatial electrochemical activity of electrodes, Anal. Chem. 73 (2001) 4229–4240.
[25] K.T. Rodolfa, A. Bruckbauer, D. Zhou, Y.E. Korchev, D. Klenerman, Two-component graded deposition of biomolecules with double-barreled nanopipette, Angew. Chem. Intl. Ed. 44 (2005) 6854–6859.
[26] K.T. Rodolfa, A. Bruckbauer, D. Zhou, A.I. Schevchuk, Y.E. Korchev, D. Klenerman, Nanoscale pipetting for controlled chemistry in small arrayed water droplets using a double-barrel pipet, Nano Lett. 2 (2006) 252–257.
[27] H. Matsuoka, S. Shimoda, Y. Miwa, M. Saito, Automatic positioning of a microinjector in mouse ES cells and rice protoplasts, Bioelectrochemistry 69 (2006) 187–192.
[28] T. Yasukawa, T. Kaya, T. Matsue, Dual imaging of topography and photosynthetic activity of a single protoplast by scanning electrochemical microscopy, Anal. Chem. 71 (1999) 4637–4641.
[29] A.R. Marchand, E. Pearlstein, A simple dual pressure–ejection system and calibration method for brief local application of drugs and modified salines, J. Neurosci. Methods 60 (1995) 99–105.
[30] O. Feinerman, E. Moses, A picoliter fountain-pen, using co-axial dual pipettes, J. Neurosci. Methods 127 (2003) 75–84.
[31] C.C. Park, H. Zhang, M. Pallavicini, J.W. Gray, F. Baehner, C.J. Park, M.J. Bissell, β1 integrin inhibitory antibody induces apoptosis of breast cancer cells, inhibits growth, and distinguishes malignant from normal phenotype in three dimensional cultures and in vivo, Cancer Res. 66 (2006) 1526–1535.
[32] Y. Torisawa, Y. Nashimoto, T. Yasukawa, H. Shiku, T. Matsue, Regulation and characterization of the polarity of cells embedded in reconstructed basement matrix using three-dimensional micro-culture system, Biotechnol. Bioeng. 97 (2007) 615–621.
[33] V.M. Weaver, O.W. Petersen, F. Wang, C.A. Larabell, P. Briand, C. Damsky, M.J. Bissell, Reversion of the malignant phenotype of human breast cells in three-dimensional culture and in vivo by integrin blocking antibodies, J. Cell. Biol. 137 (1997) 231–245.
[34] J. Debnath, S.K. Muthuswamy, J.S. Brugge, Morphogenesis and oncogenesis of MCF-10A mammary epithelial acini grown in three-dimensional basement membrane cultures, Methods 30 (2003) 256–268.
[35] Y. Nashimoto, Y. Takahashi, T. Yamakawa, Y. Torisawa, T. Yasukawa, T. Ito-Sasaki, M. Yokoo, H. Abe, H. Shiku, H. Kambara, T. Matsue, Measurement of gene expression from single adherent cells and spheroids collected using fast electrical lysis, Anal. Chem. 79 (2007) 6823–6830.

Biorheology 46 (2009) 401–415
DOI 10.3233/BIR-2009-0551
IOS Press

A versatile micro-mechanical tester for actin stress fibers isolated from cells

Tsubasa S. Matsui [a,*], Shinji Deguchi [b], Naoya Sakamoto [a], Toshiro Ohashi [a,c] and Masaaki Sato [a,b]

[a] *Department of Bioengineering and Robotics, Graduate School of Engineering, Tohoku University, Sendai, Japan*

[b] *Department of Biomedical Engineering, Graduate School of Biomedical Engineering, Tohoku University, Sendai, Japan*

[c] *Present address: Division of Human Mechanical Systems and Design, Graduate School of Engineering, Hokkaido University, Sapporo, Japan*

Received 17 May 2009
Accepted in revised form 9 September 2009

Abstract. Conventional atomic force microscopy is one of the major techniques to evaluate mechanical properties of cells and subcellular components. The use of a cantilever probe for sample manipulation within the vertical plane often makes absolute positioning of the probe, subject to thermal drift, difficult. In addition, the vertical test is unable to observe changes in the sample structure responsible for mechanical behavior detected by the probe. In the present study, an alternative mechanical tester was developed that incorporated a pair of micro-needles to manipulate a sample in a project plane, allowing acquisition of the accurate probe position and entire sample image. Using a vision-based feedback control, a micro-needle driven by a piezo actuator is moved to give user-defined displacements or forces to sample. To show its usefulness and versatility, three types of viscoelastic measurements on actin stress fibers isolated from smooth muscle cells were demonstrated: strain rate-controlled tensile tests, relaxation tests and creep tests. Fluorescence imaging of the stress fibers using Qdots over the course of the measurements, obtained through multiple image detectors, was also carried out. The technique described here is useful for examining the quantitative relationship between mechanical behavior and related structural changes of biomaterials.

Keywords: Tensile tester, visual feedback, fluorescence microscopy, cytoskeleton, stress fiber, viscoelastic properties

1. Introduction

The level of mechanical tension in a blood vessel is known to regulate vascular physiology and pathogenesis [35,41–43]. The tension in vascular smooth muscle cells is produced passively by the blood pressure and actively by actin stress fibers inside the cells. The stress fiber is a contractile cytoskeletal structure made of proteins, mainly, actin, myosin and α-actinin [9,27]. There has recently been increasing evidence suggesting that the intracellular tension in stress fibers plays a critical role in mechano-sensing and resultant vascular remodeling [13,17–19,28,29,38]. To quantitatively consider how the tension in stress fibers is borne and transmitted in the cytoplasm to induce the cellular remodeling, knowledge

*Address for correspondence: Tsubasa S. Matsui, Tohoku University, 6-6-11-1306-2 Aramaki-Aoba, Sendai 980-8579, Japan. Tel./Fax: +81 22 795 3936; E-mail: tsubasa@bml.mech.tohoku.ac.jp.

of their biorheological characteristics such as the viscoelastic properties is crucial. However, compared with increasing reports on those properties of the whole cells [4,26,44,47], the properties intrinsic to individual stress fibers remain poorly understood.

So far, several techniques that allow physical manipulation of cytoskeletal structures such as stress fibers have been developed and applied to evaluation of their mechanical properties. For instance, optical tweezers [2,6,16,21,36] enable the physical trapping of a biological sample by laser radiation pressure. A constraint of its low trapping stiffness, however, restricts the achievable generative force to an order of magnitude of pico-Newtons. Deflectable micro-cantilevers made of glass or micro-fabricated materials were also used in experiments [5,7,8,20,22–24,30,31,34,48,49,51,52]. By measuring the deflection of a micro-cantilever whose stiffness is known in advance, the loading–deformation relationship of a biomaterial can be obtained. In contrast to the narrow force range of optical tweezers, suitable design of the cantilever geometry and size enables force measurements to be made over a wide range from subpico- [30] to micro-Newton [37,39]. From the standpoint of force range, this technique is therefore more applicable to a variety of mechanical tests on biomaterials.

One main reason of the lack of experimental data on individual stress fibers seems attributable to the difficulty of the measurement. Atomic force microscopy (AFM), which utilizes a micro-fabricated cantilever, is one of the current major techniques for such mechanical tests on biological materials including measurement of the strength of protein bonds [15,45,51]. Manipulation and consequent deformation of biological materials using a conventional AFM, however, occur only within the vertical plane. This makes accurate detection of the absolute cantilever position and sample deformation very difficult, since an unexpected and often unavoidable thermal drift appears during experiment. In contrast, the use of a pair of cantilevers instead of that of a single cantilever overcomes the difficulty, as the experiment can be performed in a projected horizontal plane thereby allowing observation of the entire sample deformation [7,30,31,34,39,51].

The technique using a pair of cantilevers in a project plane has been applied to mechanical tests on cytoskeletal structures [7,8,30,31,34], whole cells [10,11,37,39,52], and other subcellular structural components [3,22]. To the best of our knowledge, the first report that described a feedback control of strain rate of living tissues at the micro-scale was provided by our group [7]. In that work, we developed a servomechanism-equipped tensile tester and demonstrated a strain rate-controlled tensile test of an in vitro stress fiber isolated from smooth muscle cells. The system that used a circular split photodiode as a cantilever detector, however, had a severe limitation in effective measurement range. Due to this limitation, we failed to use the system as a versatile apparatus allowing quantification of a variety of viscoelastic properties. Further, although recent studies have reported sophisticated apparatuses with the capability of viscoelastic characterization of whole cells [10,11], those measurements were all done under bright-field illumination. Thus, no study has yet appeared that carried out fluorescence imaging of constituent proteins during the mechanical measurements. As the relation between macroscopic mechanical properties of stress fibers and their structural constituents are largely unknown, an experimental apparatus that allows versatile mechanical tests to be made, together with the acquisition of associated structural changes detectable by imaging, should be very useful.

In the present study, a micro-tensile test system was developed that permits (i) viscoelastic measurements that are widely applicable to quantification of strain rate-dependency, relaxation and creep properties, with (ii) a wide force/displacement range by means of a pair of cantilevers and (iii) together with simultaneous observation of fluorescently-labeled constituents during the measurement. Detection of the force and displacement over such wide measurement ranges were realized using a vision-based system. Fluorescence imaging is realized by employing dichroic mirrors and multiple image detectors.